

## **Reply to reviewer n.1: M. Mergili**

“Evaluating performances of simplified physically based models for landslide susceptibility”

G. Formetta, G. Capparelli, P. Versace.

**I have seen with pleasure that the authors have responded to my suggestions in an appropriate way, so that I can now recommend the manuscript for publication.**

We thank the reviewer for the useful comments that improved the quality of our paper. We are pleased it was satisfied and we replied below, point by point, to the minor suggestions.

### **Minor suggestions**

#### **1Q. Grammar and style still have to be polished**

1A. We thank the reviewer for the suggestion. A native English speaker revised the last version of the paper. The corrections we made are presented in the back tracking version of the revised paper.




#### **2A. With regard to the methodology, I recommend to replace "objective" with "reproducible"**

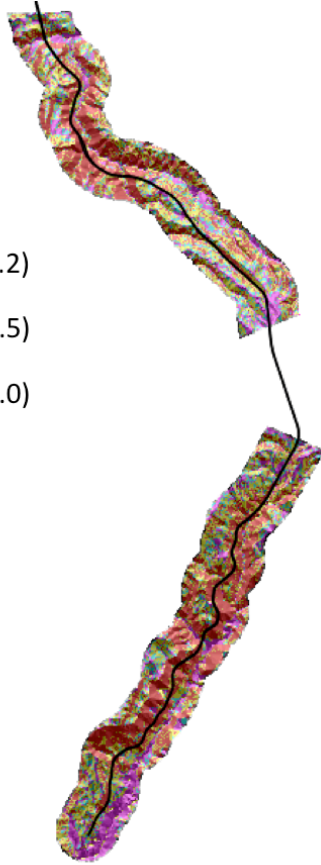
2Q. We revised according the reviewer suggestion except when is connected to “objective function”.

#### **3Q. Legend of Fig. 7: be careful, FS=1.0 and FS=2.0 are not assigned to any class**

3A. We revised the legend according the reviewer suggestion. Below you can find the revised figure:



-  Class 1 ( $FS \leq 1.0$ )
-  Class 2 ( $1.0 < FS < 1.2$ )
-  Class 3 ( $1.2 < FS < 1.5$ )
-  Class 4 ( $1.5 < FS < 2.0$ )
-  Class 5 ( $FS \geq 2.0$ )



8 Km

Unknown

Formatted: Font:(Default) Arial, Bold

## **Reply to reviewer n.2: unknown**

**“Evaluating performances of simplified physically based models for landslide susceptibility”**

**G. Formetta, G. Capparelli, P. Versace.**

**Dear authors,**

**In general the manuscript is not well arranged and reflecting the body of the manuscript. Also, the introduction section is not provides sufficient background for the readers. The manuscript in my opinion it is necessary to provide additional information and clarify some aspects in order to be accepted for publication in another journal. I think manuscript cannot be accepted for publication because have so many scientific mistakes. In the following list, there are some general suggestions need to be considered by the authors.**

We thank the reviewer for the useful comments and suggestions and we replied point by point to each of the questions he asked.

### **Specific Comments:**

**1Q Abstract: I think Abstract section has not been well written. Authors must bring obtained results and conclusion of research in end of this section. I did not see any validation method in this paper and also the condition factors in landslide occurs has been missed.**

1A. We thank the reviewer for the comment. We modified the abstract in order to underline: i) the reasons why was useful to apply the methodology in the study area, ii) the fact that we validated our models using a detailed landslide inventory map of the area, and iii) the main conclusions of our application.

New sentence:

“The area is extensively subject to rainfall-induced shallow landslides mainly because of its complex geology and climatology. The analysis was carried out

considering all the combinations of the eight optimized indices and the three models. Parameter calibration, verification, and model performance assessment were performed by a comparison with a detailed landslide inventory map for the area. The results showed that the index distance to perfect classification in the receiver operating characteristic plane (D2PC) coupled with model M3 is the best modeling solution for our test case.”

**2Q Introduction: This section also is general. Considering high frequency of landslides, there is a big demand to prepare quality landslide susceptibility maps over the world. Different kinds of techniques are available including LSM. I miss in your paper some summarization of approaches used for landslide susceptibility. Please provide some comparison of methods and try to evaluate the advantages and disadvantages of your method in Introduction section.**

2A. We thank the reviewer for the suggestion. In the introduction we added the following sentences to introduce how other landslide susceptibility methods works and to compare strength and limitations of different approaches. The new sentences are:

“Bivariate statistical methods ignore the interdependence of instability factors whereas multivariate analysis is able to statistically consider their interactions. Other data-driven methods for landslide susceptibility analysis include the use of neural networks (Pradhan, 2011; Conforti et al., 2014), support vector machines (Pradhan, 2013 and citations therein), and Bayesian networks (Lee et al., 2002)

“One of the main advantages of data-driven methods for landslide susceptibility is that they can be easily applied in wide areas while deterministic models are in general applied in local analyses. The latter are more computationally expensive and require detailed input data and parameters, which often involve high uncertainty. On the other hand, data-driven methods assume that landslides are caused by the same combination of instability factors overall the study area, whereas deterministic models enable different triggering mechanisms to be understood and investigated”

**3Q. Please provide additional information about other studies that use Object Modeling System in landslide analysis. A paragraph concerning the different approach used in the present study would be useful. Actually the end of introduction section belong to the purpose of study. Authors must mention here aims of study clearly. I did not see this note and this important note was missing. Please highlight your contribution and novelty in this section.**

3A. We thank the reviewer for the suggestions. We actually split this question in two parts:

- "Please provide additional information about other studies that use Object Modeling System in landslide analysis. A paragraph concerning the different approach used in the present study would be useful". To answer to this question we specified the different approaches used in OMS for landslide modeling. To this purpose we added the following questions with the aim of clarify to the reader that no previous work were finalized to landslide early warning and not to landslide susceptibility assessment. The new sentence is: "The OMS framework has been previously used as the core for landslides modeling (Formetta et al., 2016; Formetta et al., 2015). These studies deal with real time early warning systems for landslide risks and involve 3D physically based hydrological modeling of very small catchments (up to around 20 km<sup>2</sup>). In contrast, the current application focuses on wider areas landslide susceptibility assessments using completely different physically based models which are presented in the next section."

Moreover in the text we tried to specify the differences respect to other studies in the following sentence:

"The methodology presented in this paper for landslide susceptibility analysis (LSA) represents one model configuration within the more general NewAge-JGrass system. It includes two new models specifically developed for this paper: mathematical components for landslide susceptibility mapping and procedures for landslides susceptibility model verification and selection."

- "Actually the end of introduction section belong to the purpose of study. Authors must mention here aims of study clearly. I did not see this note and

this important note was missing. Please highlight your contribution and novelty in this section”

- We thank the reviewer for the suggestion. We modified the old sentence in which we explained the novelty of the paper, which was:

Old sentence: “For a generic landslide susceptibility component it is possible to estimate the model parameters that optimize a given GOF metric. To perform this step the user can choose between a set of GOF indices and a set of automatic calibration algorithms. Comparing the results obtained for different models and for different GOF metrics the user can select the most performing combination for his or her own case study.”

In the revised paper we specified in bullet form both the novelties of the paper and the reasons for which the procedure that we propose will be useful for the end-user:

New sentence: “Unlike previous applications, our methodology aims to objectively: i) select a set of the most appropriate OFs in order to determine the best model parameters; ii) compare the performance of a model using the parameter sets selected in the previous step in order to identify the OFs that provides particular and not redundant information; iii) perform a model parameter sensitivity analysis in order to understand the relative importance of each parameter and its influence on the model performance. The methodology enables the user to: i) identify the most appropriate OFs for estimating the model parameters and ii) compare different models in order to select the best one that estimates the landslide susceptibility of the study area.”

#### **4Q. MODELING FRAMEWORK:**

**Is it not better bring this section in under Material and methods section?**

4A. we agree with the reviewer comment. We modified the title of the section 2 in Material and Methods, which now include the following subsections: modeling framework, landslide susceptibility models, automatic calibration and model verification procedure, and site description.

#### **5Q. Site Description**

**Please provide more information about the morphometric, tectonic settings of the research area. Also provide additional information about the types of landslides encountered in the study area. This information would enable the reader clearly understand the instability problems of the research area.**

5A: We thank the reviewer for the suggestion. We tried to specify the morphology and tectonic setting of the area in the following sentence:

“The test site was located in Calabria, Italy, along the Salerno-Reggio Calabria highway between Cosenza and Altilia municipalities, in the southern part of the Crati basin (Figure 2). The mean annual precipitation is about of 1200 mm, distributed over approximately 100 rainy days, with a mean annual temperature of 16 °C. Rainfall peaks occur from October to March, when mass wasting and severe water erosion processes are triggered (Capparelli et al., 2012, Conforti et al., 2011, Iovine et al., 2010).

In the study area the topographic elevation has an average value of around 450 m a.s.l., with a maximum value of 730 m a.s.l. Slopes, computed from the 10 meters resolution digital elevation model, range from 0° to 55°, while the average is about 26°.

The Crati Basin is a Pleistocene-Holocene extensional basin filled by clastic marine and fluvial deposits (Vezzani, 1968; Colella et al., 1987; Fabbri et al., 2014). The stratigraphic succession of the Crati Basin can be simply divided into two sedimentary units as suggested by Lanzafame and Tortorici (1986). The first unit is a Lower Pliocene succession of conglomerates and sandstones passing upward into a silty clay (Lanzafame and Tortorici, 1986) second unit. This is a series of clayey deposits grading upward into sandstones and conglomerates which refer to Emilian and Sicilian, respectively (Lanzafame and Tortorici, 1986), as also suggested by data provided by Young and Colella (1988). ”

Moreover in the revised part of the paper we added more information about the tectonic setting of the analyzed area and about the soil type classification that, as specified by the reviewer, was missing:

New sentence: “In the study area the second unit outcrops. A topsoil of about 1.5 - 2.0 m lies on sandy-gravelly and sandy deposits, which are generally well-stratified. Soils range from Alfisols (i.e. highly mature soils) to Inceptisols

and Entisols (i.e. poorly developed soils). Due to the combination of such climatic, geo-structural, and geomorphological features the test site is one of the most landslide prone areas in Calabria (Conforti et al., 2014; Carrara and Merenda, 1976; Iovine et al., 2006,).”

#### **6Q. Models performances correlations assessment**

**Authors fail to adequately provide a critical discussion as to the limitations of their study. The entire mention section is dedicated to highlighting the strengths of the method over previous approaches. However, it is absolutely vital that you clearly present and address the limitations of the proposed method, of which I feel there are several notable points. Given the context of the paper and the suggestion that this method could be used by decision-makers it is vital that you are clear and explicit about its potential uses as well as its limitations - such information is crucial to ensure decision-makers are adequately informed.**

6A: We thank the reviewer for the comments. In the revised paper we have specified the limitations of the methodology and the modeling approach. In particular we added the following sentences in the section Results and Discussion:

Subsection: “Models calibration and verification”

“Finally, is important to consider the limitation of the models used for the current applications. The models M1 and M2 are not able to mimic the transient nature of the precipitation and infiltration processes and only M3 is able to account for the combined effect of storm duration and intensity in the triggering mechanism. Moreover, in this study we neglected effects such as spatial rainfall variability, roads, and other engineering works.”

Subsection ” Models sensitivity assessment”:

“Finally, it is important to consider that the methodology used for evaluating the parameter sensitivity is based on changing the parameters one-at-time. Although this procedure facilitates an inter-comparison of the results (because the parameter sensitivity is computed with reference to the optimal parameter set), it does not take into account simultaneous variations or interactions between parameters.”



**7QI did not see Results and Discussion section in your manuscript? In this authors must bring obtained results of study here clearly without any generalization. This section is essential section in scientific papers.**

7A: We thank the reviewer for the suggestion. In the revised paper the section 3 is extended and named Results and Discussion because in this section we presented and commented (adding the useful reviewer's requests) our results. Respect to the previous version of the paper we: i) added more discussions on the results and ii) provided in a more explicit form some of the limitations of our study (see 6A)

**8Q. Conclusion: This section was not well written because I did not see concluded notes about this research here. Authors must rewrite this section.**

8A. We thank the reviewer for the suggestions. We rearranged the entire section and we added two main sentences. The first sentence aims to stress the objectives of the methodology presented in the paper:

“The first step identifies the more appropriate OFs for the model parameter optimization. The second step verifies the information content of each optimized OF, checking whether it is analogous to other metrics or peculiar to the optimized OF. Finally the last step quantifies the relative influence of each model parameter on the model performance.”

The second sentence aims to better clarify in bullet form the conclusions provided by the application:

“The procedure was applied in a test case on the Salerno-Reggio Calabria highway and led to the following conclusions: 1) the OFs AI, D2PC, SI, and TSS coupled with the models M2 and M3 provided the best performances among the eights metrics used in the calibration; 2) the four selected OFs provided quite similar model performances in terms of MP vectors, i.e. one of them would be sufficient for the model application; 3) M3 showed the best performance by optimizing the D2PC index. In fact M3 responded to parameter variations with changes in model performances.”

# Evaluating Performances of Simplified Physically Based Models for Landslide Susceptibility.

Giuseppe Formetta, Giovanna Capparelli and Pasquale Versace

University of Calabria Dipartimento di Ingegneria Informatica, Modellistica, Elettronica e Sistemistica Ponte Pietro Bucci, cubo 41/b, 87036 Rende, Italy  
([giuseppe.formetta@unical.it](mailto:giuseppe.formetta@unical.it), [giovanna.capparelli@unical.it](mailto:giovanna.capparelli@unical.it), [pasquale.versace@unical.it](mailto:pasquale.versace@unical.it))

**Abstract:** Rainfall induced shallow landslides can lead to loss of life and significant damage to private and public properties, and transportation systems, etc. Predicting locations that might be susceptible to shallow landslides is a complex task and involves many disciplines: hydrology, geotechnical science, geology, hydrogeology, geomorphology, and statistics. Two main approaches are commonly used: statistical or physically based models. Reliable model applications involve automatic parameter calibration, objective quantification of the quality of susceptibility maps, and model sensitivity analyses. This paper presents a methodology to systemically and objectively calibrate, verify and compare different models and model performance indicators in order to identify and select the models whose behaviors are the most reliable for particular case studies.

The procedure was implemented in a package of models for landslide susceptibility analysis and integrated in the NewAge-JGrass hydrological model. The package includes three simplified physically based models for landslide susceptibility analysis (M1, M2, and M3) and a component for model verification. It computes eight goodness of fit indices by comparing pixel-by-pixel model results and measurement data. The integration of the package in NewAge-JGrass uses other components such as geographic information system tools to manage input-output processes, and automatic calibration algorithms to estimate model parameters.

The system was applied for a case study in Calabria (Italy) along the Salerno-Reggio Calabria highway, between Cosenza and Altìlia. The area is extensively subject to rainfall-induced shallow landslides mainly because of its complex geology and

Giuseppe Formetta 10/21/2016 2:50 PM

Deleted: cause ...ead to loss of life ... [1]

Giuseppe Formetta 10/21/2016 2:55 PM

Deleted: ...ased models for ... [2]

Giuseppe Formetta 10/21/2016 2:58 PM

Deleted: municipality

67 climatology. The analysis was carried out considering all the combinations of the  
 68 eight optimized indices and the three models. Parameter calibration, verification, and  
 69 model performance assessment were performed by a comparison with a detailed  
 70 landslide inventory map for the area. The results showed that the index distance to  
 71 perfect classification in the receiver operating characteristic plane (D2PC) coupled  
 72 with model M3 is the best modeling solution for our test case.

73

74 **Keywords:** Landslide modelling; Object Modeling System; Models calibration.

75

## 76 1 INTRODUCTION

77

78 Landslides are one of the main dangerous geo-hazards worldwide and constitute a  
 79 serious menace for public safety leading to human and economic losses (Park  
 80 2011). Geo-environmental factors such as geology, land-use, vegetation, climate,  
 81 and increasing populations may increase the occurrence of landslides (Sidle and  
 82 Ochiai 2006). Landslide susceptibility assessments, i.e. the likelihood of a landslide  
 83 occurring in an area on the basis of local terrain conditions (Brabb, 1984), is not only  
 84 crucial for an accurate landslide hazard quantification but also a fundamental tool for  
 85 the environmental preservation and responsible urban planning (Cascini et al.,  
 86 2005).

87 Many methods for landslide susceptibility mapping have been developed and can be  
 88 grouped in two main branches: qualitative and quantitative methods (Glade and  
 89 Crozier, 2005; Corominas et al., 2014 and references therein).

90 Qualitative methods, based on field campaigns and expert knowledge and  
 91 experience, are subjective but necessary to validate quantitative method results.

92 Quantitative methods include statistical and physically based methods. Statistical  
 93 methods (e.g. Naranjo et al., 1994; Chung et al. 1995; Guzzetti et al., 1999; Catani  
 94 et al., 2005) use different approaches such as bivariate statistics, multivariate  
 95 analysis, discriminant analysis, random forest to link instability factors (such as  
 96 geology, soil, slope, curvature, and aspect) with past and present landslides.

97 Bivariate statistical methods ignore the interdependence of instability factors  
 98 whereas multivariate analysis is able to statistically consider their interactions. Other  
 99 data-driven methods for landslide susceptibility analysis include the use of neural

Giuseppe Formetta 10/6/2016 5:05 PM

Deleted: provided ...as carried out ... [3]

Giuseppe Formetta 10/21/2016 3:00 PM

Deleted: major ...ain worldwide ... [4]

Giuseppe Formetta 10/21/2016 3:09 PM

Deleted: During the last few decad ... [5]

Giuseppe Formetta 10/21/2016 3:10 PM

Deleted: on the basis of ...xpert ... [6]

130 networks (Pradhan, 2011; Conforti et al., 2014), support vector machines (Pradhan,  
 131 2013 and citations therein), and Bayesian networks (Lee et al., 2002). Deterministic  
 132 models (e.g. Montgomery and Dietrich, 1994; Lu and Godt, 2008; Borga et al., 2002;  
 133 Simoni et al., 2008; Capparelli and Versace, 2011; Lu and Godt, 2013) synthesize  
 134 the interaction between hydrology, geomorphology, and soil mechanics in order to  
 135 physically understand and predict the location and timing that trigger landslides.  
 136 These models generally include a hydrological and a slope stability component. The  
 137 hydrological component simulates infiltration and groundwater flow processes with  
 138 different degrees of simplification, from steady state (e.g. Montgomery and Dietrich,  
 139 1994) to transient analyses (Simoni et al., 2008). The soil-stability component  
 140 simulates the slope safety factor (FS) defined as the ratio of stabilizing to  
 141 destabilizing forces. One of the main advantages of data-driven methods for  
 142 landslide susceptibility is that they can be easily applied in wide areas while  
 143 deterministic models are in general applied in local analyses. The latter are more  
 144 computationally expensive and require detailed input data and parameters, which  
 145 often involve high uncertainty. On the other hand, data-driven methods assume that  
 146 landslides are caused by the same combination of instability factors overall the study  
 147 area, whereas deterministic models enable different triggering mechanisms to be  
 148 understood and investigated.

149 The results of a landslide susceptibility analysis strongly depend on the model  
 150 hypothesis, parameter values, and parameter estimation method. Questions  
 151 regarding the performance evaluation of the landslide susceptibility model, the  
 152 choice of the best accurate model, and the selection of the best performing method  
 153 for parameter estimation are still open. Thus, is needed a procedure that facilitates  
 154 reproducible comparisons between different models and evaluation criteria aimed at  
 155 the selection of the most accurate models.

156 Much effort has been devoted to the crucial problem of evaluating landslide  
 157 susceptibility model performances (e.g. Dietrich et al., 2001; Frattini et al., 2010, and  
 158 Guzzetti et al., 2006). Accurate discussions about the most common quantitative  
 159 measures of goodness of fit (GOF) between measured and modeled data are  
 160 discussed in Bennet et al., (2013), Jolliffe and Stephenson, (2012), Beguería (2006),  
 161 Brenning (2005) and references therein. We have summarized them in Appendix 1.  
 162 Usually one of these indices is selected and used as an objective function (OF) in

Giuseppe Formetta 10/1/2016 1:15 PM

Deleted: .

... [7]

Giuseppe Formetta 10/21/2016 3:18 PM

Deleted: R...sults of a landslide

... [8]

Giuseppe Formetta 10/21/2016 3:21 PM

Deleted: Many ...uch efforts...wer

... [9]

Giuseppe Formetta 10/3/2016 7:33 PM

Formatted

... [10]

201 combination with a calibration algorithm in order to obtain the optimal set of model  
 202 parameters. However, in most cases the selection of the OF is not justified or  
 203 compared with other options.

Giuseppe Formetta 10/3/2016 7:33 PM  
 Formatted ... [11]

204 The wrong classifications in landslide susceptibility analysis not only risk a loss of life  
 205 but also have economic consequences. For example locations classified as stable  
 206 increase their economical value because no construction restrictions will be applied,  
 207 while the reverse is true for locations classified as unstable.

Giuseppe Formetta 10/21/2016 3:26 PM  
 Deleted: Wrong classifications in ... [12]

208 In this work we propose an objective methodology for environmental model analysis  
 209 which selects the best performing model based on a quantitative comparison and  
 210 assessment of model prediction skills. In this paper the methodology is applied to  
 211 assess the performances of simplified landslide susceptibility models. As the  
 212 procedure is model independent, it can be used to assess the ability of any type of  
 213 environmental model to simulate natural phenomena.

Giuseppe Formetta 10/21/2016 3:28 PM  
 Deleted: s...analysis that allows t... [13]

214 Unlike previous applications, our methodology aims to objectively: i) select a set of  
 215 the most appropriate OFs in order to determine the best model parameters; ii)  
 216 compare the performance of a model using the parameter sets selected in the  
 217 previous step in order to identify the OFs that provides particular and not redundant  
 218 information; iii) perform a model parameter sensitivity analysis in order to understand  
 219 the relative importance of each parameter and its influence on the model  
 220 performance. The methodology enables the user to: i) identify the most appropriate  
 221 OFs for estimating the model parameters and ii) compare different models in order to  
 222 select the best one that estimates the landslide susceptibility of the study area.

Giuseppe Formetta 10/3/2016 8:38 PM  
 Formatted: Normal

223 The procedure is implemented in the open source and GIS based hydrological  
 224 model, denoted as NewAge-JGrass (Formetta et al., 2014) which uses the Object  
 225 Modeling System (OMS, David et al., 2013) modeling framework. OMS is a Java  
 226 based modeling framework which promotes the idea of programming by components.  
 227 It provides the model developers with many features such as: multithreading, implicit  
 228 parallelism, models interconnection, and a GIS based system.

Giuseppe Formetta 10/21/2016 3:37 PM  
 Deleted: that ...hich uses the Obj... [14]

Giuseppe Formetta 10/3/2016 8:39 PM  
 Formatted: Font:(Default) Arial

Giuseppe Formetta 10/21/2016 3:37 PM  
 Deleted: that

Giuseppe Formetta 10/3/2016 8:39 PM  
 Formatted: Font:(Default) Arial

Giuseppe Formetta 10/21/2016 3:37 PM  
 Deleted: and

229 The NewAge-JGrass system, Fig. 1, contains models, automatic calibration  
 230 algorithms for model parameter estimation, and methods for estimating the  
 231 goodness of the models prediction. The open source GIS uDig  
 232 (<http://udig.refractor.net/>) and the uDig-Spatial Toolbox (Abera et al., (2014),  
 233 <https://code.google.com/p/jgrasstools/wiki/JGrassTools4udig>) are used as a

Giuseppe Formetta 10/3/2016 8:39 PM  
 Formatted: Font:(Default) Arial

Giuseppe Formetta 10/21/2016 3:38 PM  
 Deleted: facilitates

Giuseppe Formetta 10/3/2016 8:39 PM  
 Formatted ... [15]

Giuseppe Formetta 10/21/2016 3:38 PM  
 Deleted: e... ewAge-JGrass sy... [16]

263 visualization and input/out data management system. The OMS framework has been  
 264 previously used as the core for landslides modeling (Formetta et al., 2016; Formetta  
 265 et al., 2015). These studies deal with real time early warning systems for landslide  
 266 risks and involve 3D physically based hydrological modeling of very small  
 267 catchments (up to around 20 km<sup>2</sup>). In contrast, the current application focuses on  
 268 wider areas landslide susceptibility assessments using completely different  
 269 physically based models which are presented in the next section.  
 270 The methodology presented in this paper for landslide susceptibility analysis (LSA)  
 271 represents one model configuration within the more general NewAge-JGrass  
 272 system. It includes two new models specifically developed for this paper:  
 273 mathematical components for landslide susceptibility mapping and procedures for  
 274 landslides susceptibility model verification and selection. The LSA configuration also  
 275 uses two models that have already been implemented in NewAge-JGrass: the  
 276 geomorphological model set-up and the automatic calibration algorithms for model  
 277 parameter estimation. All the models used in the LSA configuration are presented in  
 278 Fig. 1, encircled with a dashed red line.  
 279 The methodology is presented in section 2. It was setup considering three different  
 280 landslide susceptibility models, eight GOF metrics, and one automatic calibration  
 281 algorithm. The flexibility of the system enables more models, and GOF metrics to be  
 282 added, and different calibration algorithms can be used. Thus deferent LSA  
 283 configurations can be created depending on: the landslide susceptibility model, the  
 284 calibration algorithm, and the GOFs selected by the user. Finally, Section 3 presents  
 285 a case study of landslide susceptibility mapping along the A3 Salerno-Reggio  
 286 Calabria highway in Calabria, which illustrates the capability of the system.

## 2 MATERIALS AND METHODS

### 2.1 Modelling Framework

291  
 292 The landslide susceptibility analysis (LSA) is implemented in the context of NewAge-  
 293 JGrass (Formetta et al., 2014), an open source large-scale hydrological modeling  
 294 system. It models the whole hydrological cycle: water balance, energy balance, snow  
 295 melting, etc. (Figure 1). The system implements hydrological models, automatic

Giuseppe Formetta 10/1/2016 4:05 PM  
**Formatted:** Superscript

Giuseppe Formetta 10/21/2016 3:40 PM  
**Deleted:** into

Giuseppe Formetta 10/21/2016 3:40 PM  
**Deleted:** Moreover

Giuseppe Formetta 10/2/2016 9:36 AM  
**Deleted:** For a generic landslide susceptibility component it is possible to estimate the model parameters that optimize a given GOF metric. To perform this step the user can choose between a set of GOF indices and a set of automatic calibration algorithms. Comparing the results obtained for different models and for deferent GOF metrics the user can select the most performing combination for his or her own case study .

Giuseppe Formetta 10/21/2016 3:42 PM  
**Formatted:** Default

Giuseppe Formetta 10/21/2016 3:41 PM  
**Deleted:** , accurately

Giuseppe Formetta 10/21/2016 3:41 PM  
**Deleted:** ,

Giuseppe Formetta 10/21/2016 3:41 PM  
**Deleted:** allows

Giuseppe Formetta 10/21/2016 3:41 PM  
**Deleted:** to add

Giuseppe Formetta 10/21/2016 3:42 PM  
**Deleted:** to use

Giuseppe Formetta 10/21/2016 3:42 PM  
**Deleted:** realized

Giuseppe Formetta 10/3/2016 8:39 PM  
**Deleted:** ... [17]

Giuseppe Formetta 10/3/2016 8:39 PM  
**Formatted:** Font:(Default) Arial

Giuseppe Formetta 10/3/2016 8:39 PM  
**Formatted:** Font:(Default) Arial

Giuseppe Formetta 10/21/2016 3:42 PM  
**Deleted:** s

Giuseppe Formetta 10/3/2016 8:39 PM  
**Formatted:** Font:(Default) Arial

Giuseppe Formetta 10/21/2016 3:43 PM  
**Deleted:** that

Giuseppe Formetta 10/3/2016 8:39 PM  
**Formatted:** Font:(Default) Arial

Giuseppe Formetta 10/2/2016 9:45 AM  
**Formatted:** Font:Bold

Giuseppe Formetta 10/2/2016 9:45 AM  
**Formatted:** Font:Bold

Giuseppe Formetta 10/2/2016 9:43 AM  
**Deleted:** . MODELING

Giuseppe Formetta 10/2/2016 9:45 AM  
**Deleted:** FRAMEWORK

321 calibration algorithms for model parameter optimization, and evaluation, and a GIS  
 322 for input output visualization, (Formetta et al., 2011, Formetta et al., 2014). NewAge-  
 323 JGrass is a component-based model. Each hydrological process is described by a  
 324 model (energy balance, evapotranspiration, run off production in figure 1). Each  
 325 model implements one or more components, (considering for example the model  
 326 evapotranspiration in Figure 1, the user can select between three different  
 327 components: Penman-Monteith, Priestly-Taylor, and Fao). In addition, each  
 328 component can be linked to the others and executed at runtime, this building a  
 329 model configuration. Figure 1 offers a complete picture of the system and the  
 330 integration of the new LSA configuration encircled with dashed red lines. More  
 331 precisely the LSA in the current configuration includes two new models: a landslides  
 332 susceptibility model and a verification and selection model. The first includes three  
 333 components proposed in Montgomery and Dietrich, 1994, Park et al., 2013, and  
 334 Rosso et al., 2006, the latter includes the “three step verification procedure” (3SVP),  
 335 presented in Section 2. The LSA configuration also includes another two models  
 336 previously implemented in the NewAge-JGrass system: i) the Horton Machine for  
 337 geomorphological model setup which computes input maps such as slope and total  
 338 contributing area and which displays the model's results, and ii) the particle swarm  
 339 for automatic calibration. Subsection 2.1 presents the landslide susceptibility model  
 340 and 2.2 presents the model selection procedure (3SVP).

341

## 342 2.2. Landslide susceptibility models

343

344 The landslide susceptibility models implemented in NewAge-JGrass and presented  
 345 in a preliminary application in Formetta et al., 2015 consist of the Montgomery and  
 346 Dietrich (1994) model (M1), the Park et al. (2013) model (M2) and the Rosso et al.  
 347 (2006) model (M3). The three models derive from simplifications of the infinite slope  
 348 equation (Grahm J., 1984, Rosso et al., 2006, Formetta et al., 2014) for the factor of  
 349 safety:

350

$$351 \quad FS = \frac{C \cdot (1+e)}{\left[ G_s + e \cdot S_r + w \cdot e \cdot (1-S_r) \right] \cdot \gamma_w \cdot H \cdot \sin \alpha \cdot \cos \alpha} + \frac{\left[ G_s + e \cdot S_r - w \cdot (1+e \cdot S_r) \right] \cdot \tan \varphi'}{\left[ G_s + e \cdot S_r + w \cdot e \cdot (1-S_r) \right] \cdot \tan \alpha} \quad (1)$$

352

Giuseppe Formetta 10/21/2016 3:43 PM

Deleted: :

Giuseppe Formetta 10/21/2016 3:43 PM

Deleted: e

Giuseppe Formetta 10/21/2016 3:43 PM

Deleted: ;

Giuseppe Formetta 10/21/2016 3:43 PM

Deleted: e

Giuseppe Formetta 10/3/2016 8:43 PM

Deleted: (

Giuseppe Formetta 10/3/2016 8:43 PM

Deleted: )

Giuseppe Formetta 10/21/2016 3:44 PM

Deleted: f

Giuseppe Formetta 10/21/2016 3:44 PM

Deleted: ;

Giuseppe Formetta 10/21/2016 3:45 PM

Deleted: actual

Giuseppe Formetta 10/21/2016 3:45 PM

Deleted: model for model

Giuseppe Formetta 10/21/2016 3:45 PM

Deleted: T

Giuseppe Formetta 10/21/2016 3:46 PM

Deleted: s

Giuseppe Formetta 10/21/2016 3:46 PM

Deleted: accurately

Giuseppe Formetta 10/21/2016 3:46 PM

Deleted: s

Giuseppe Formetta 10/21/2016 3:46 PM

Deleted: Moreover

Giuseppe Formetta 10/21/2016 3:47 PM

Deleted: beforehand

Giuseppe Formetta 10/21/2016 3:47 PM

Deleted: that

Giuseppe Formetta 10/21/2016 3:47 PM

Deleted: ,

Giuseppe Formetta 10/21/2016 3:47 PM

Deleted: visualize

Giuseppe Formetta 10/21/2016 3:47 PM

Deleted: P

Giuseppe Formetta 10/21/2016 3:47 PM

Deleted: S

Giuseppe Formetta 10/21/2016 3:48 PM

Deleted: subsection

Giuseppe Formetta 10/2/2016 9:43 AM

Deleted: 1

Giuseppe Formetta 10/21/2016 3:48 PM

Deleted: are:

Giuseppe Formetta 10/21/2016 3:49 PM

Deleted: s

378 where FS [-] is the factor of safety,  $C=C'+C_{root}$  is the sum of  $C_{root}$ , the root strength  
 379 [kN/m<sup>2</sup>] and  $C'$  the effective soil cohesion [kN/m<sup>2</sup>],  $\varphi'$  [-] is the internal soil friction  
 380 angle,  $H$  is the soil depth [m],  $\alpha$  [-] is the slope angle,  $\gamma_w$  [kN/m<sup>3</sup>] is the specific  
 381 weight of water, and  $w=h/H$  [-] where  $h$  [m] is the water table height above the failure  
 382 surface [m],  $G_s$  [-] is the specific gravity of soil,  $e$  [-] is the average void ratio and  $S_r$   
 383 [-] is the average degree of saturation.

384 The model M1 assumes a hydrological steady-state, flow occurring in the direction  
 385 parallel to the slope and neglect cohesion, degree of soil saturation and void ratio. It  
 386 computes  $w$  as:

$$388 \quad w = \frac{h}{H} = \min\left(\frac{Q}{T} \cdot \frac{TCA}{b \cdot \sin \alpha}, 1.0\right) \quad (2)$$

389 where  $T$  [L<sup>2</sup>/T] is the soil transmissivity defined as the product of the soil depth and  
 390 the saturated hydraulic conductivity,  $b$  [L] is the length of the contour line.  
 391 Substituting eq. (2) in (1) the model is solved for  $Q/T$  assuming  $FS=1$  and stable and  
 392 unstable sites are defined using threshold values on  $\log(Q/T)$  (Montgomery and  
 393 Dietrich, 1994).

395 Unlike M1, the model M2 considers: i) the effect of the degree of soil saturation ( $S_r$  [-]  
 396 ) and void ratio ( $e$  [-]) above the groundwater table and ii) the stabilizing contribution  
 397 of the soil cohesion. The model output is a map of safety factors (FS) for each pixel  
 398 of the analyzed area.

399 The component (M3) considers both the effects of rainfall intensity and duration on  
 400 the landslide triggering process. The term  $w$  depends on rainfall duration and is  
 401 obtained by coupling the conservation of mass of soil water with the Darcy's law  
 402 (Rosso et al., 2006) providing:

$$404 \quad w = \begin{cases} \frac{Q}{T} \cdot \frac{TCA}{b \cdot \sin \alpha} \left[ 1 - \exp\left(-\frac{e+1}{e \cdot (1-S_r)} \cdot \frac{t}{T} \cdot \frac{TCA}{b \cdot \sin \alpha} \cdot H\right) \right] & \text{if } \frac{t}{T} \cdot \frac{TCA}{b \cdot \sin \alpha} \cdot H \leq -\frac{e \cdot (1-S_r)}{1+e} \cdot \ln\left(1 - \frac{T \cdot b \cdot \sin \alpha}{TCA \cdot Q}\right) \\ 1 & \text{if } \frac{t}{T} \cdot \frac{TCA}{b \cdot \sin \alpha} \cdot H > -\frac{e \cdot (1-S_r)}{1+e} \cdot \ln\left(1 - \frac{T \cdot b \cdot \sin \alpha}{TCA \cdot Q}\right) \end{cases} \quad (3)$$

405

Giuseppe Formetta 10/21/2016 3:50 PM  
 Deleted: ,

Giuseppe Formetta 10/21/2016 3:51 PM  
 Deleted: Differently

Giuseppe Formetta 10/21/2016 3:51 PM  
 Deleted: from

Giuseppe Formetta 10/21/2016 3:51 PM  
 Deleted: e

Giuseppe Formetta 10/21/2016 3:51 PM  
 Deleted: it



411 | These models are suitable for shallow translational landslides controlled by  
 412 | groundwater flow convergence. Shallow landslides usually have a very low ratio  
 413 | between the maximum depth (D) and the length (L) of scar ( $D/L < 0.1$ , Casadei et al.,  
 414 | 2003), involve a small volume of the colluvial soil mantle and present a generally  
 415 | translational failure mechanism (Milledge et al., 2014).

416 | Each component has a user interface which specifies the input and output. Model  
 417 | inputs are computed in the GIS uDig integrated in the NewAge-JGrass system by  
 418 | using the Horton Machine package for terrain analysis (Abera et al., 2014). Model  
 419 | output maps are directly imported in the GIS and are available for the user's  
 420 | visualization.

421 | The models that we implemented present an increasing degree of complexity in  
 422 | terms of the theoretical assumptions for modeling landslide susceptibility. Moving  
 423 | from M1 to M2, the soil cohesion and soil properties were considered, and moving  
 424 | from M2 to M3 rainfall of finite duration was used.

425

### 426 | 2.3. Automatic calibration and model verification procedure

427

428 | In order to assess the models' performance we developed a model that computes  
 429 | the most common indices for assessing the quality of a landslide susceptibility map.

430 | These indices are based on a pixel-by-pixel comparison between the observed  
 431 | landslide map (OL) and predicted landslides (PL). They are binary maps with  
 432 | positive pixels corresponding to "unstable" ones, and negative pixels that correspond  
 433 | to "stable" ones. Therefore, four types of outcomes are possible for each cell. A pixel

434 | is a true-positive (tp) if it is mapped as "unstable" both in OL and in PL, which is a  
 435 | correct alarm with well predicted landslide. A pixel is a true-negative (tn) if it is

436 | mapped as "stable" both in OL in PL, which corresponds to a well predicted stable  
 437 | area. A pixel is a false-positive (fp) if it is mapped as "unstable" in PL, but is "stable"  
 438 | in OL; that is a false alarm. A pixel is a false-negative (fn) if it is mapped as "stable"  
 439 | in PL, but is "unstable" in OL, that is a missed alarm. The concept of the Receiver

440 | Operator Characteristic (ROC, Goodenough et al., 1974) graph is based on the  
 441 | values assumed by tp, fp, tn. ROCs are used to assess the performance of models

442 | which provides results assigned to one of two classes. The ROC graph is widely  
 443 | used in many scientific fields such as medicine (Goodenough et al., 1974),

Giuseppe Formetta 10/21/2016 3:51 PM  
Deleted: o

Giuseppe Formetta 10/21/2016 3:52 PM  
Deleted: on

Giuseppe Formetta 10/2/2016 9:43 AM  
Deleted: 2

Giuseppe Formetta 10/21/2016 3:53 PM  
Deleted: used

Giuseppe Formetta 10/21/2016 3:54 PM  
Deleted: that

Giuseppe Formetta 10/21/2016 3:54 PM  
Deleted: that

Giuseppe Formetta 10/21/2016 3:55 PM  
Deleted: t

Giuseppe Formetta 10/21/2016 3:55 PM  
Deleted: The

Giuseppe Formetta 10/21/2016 3:55 PM  
Deleted: is a methodology

Giuseppe Formetta 10/21/2016 3:55 PM  
Deleted: to

Giuseppe Formetta 10/21/2016 3:55 PM  
Deleted: that

455 | biometrics (Pepe, 2003) and machine learning (Provost and Fawcett, 2001). The  
 456 | ROC graph is a Cartesian plane with the FPR on the x-axis and TPR on the y-axis.  
 457 | FPR is the ratio between false positives and the sum of false positives and true  
 458 | negatives, and TPR is the ratio between true positives and the sum of true positives  
 459 | and false negatives. They are defined in Table 1 and commented on Appendix 1.  
 460 | The performance of a perfect model corresponds to the point P(0,1) on the ROC  
 461 | plane. Points that fall on the bisector (black solid line, on the plots) are associated  
 462 | with models that are considered as random: they predict stable or unstable cells with  
 463 | the same rate.  
 464 | Eight GOF indices for the quantification of model performances were implemented in  
 465 | the system. Table (1) shows their definition, range, and optimal values. A more  
 466 | comprehensive description of the indices is provided in Appendix 1.  
 467 | Automatic calibration algorithms implemented in NewAge-JGrass as OMS  
 468 | components can be used in order to tune the model parameters in order to  
 469 | reproduce the actual landslides. This is possible because each model is an OMS  
 470 | component and can be linked to the calibration algorithms as it is, without rewriting  
 471 | or modifying its code. Three calibration algorithms are embedded in the system core:  
 472 | Luca (Hay et al., 2006), a step-wise algorithm based on shuffled complex evolution  
 473 | (Duan et al., 1992), Particle Swarm Optimization (PSO), a genetic model presented  
 474 | in (Kennedy and Eberhart, 1995), and DREAM (Vrugt et al., 2008) an acronym for  
 475 | Differential Evolution Adaptive Metropolis. In the actual configuration we used a  
 476 | Particle Swarm Optimization (PSO) algorithm to estimate optimal values of the  
 477 | model parameters.  
 478 | During the calibration procedure, the selected algorithm compares the model output  
 479 | in terms of a binary map (stable or unstable pixel) with the actual landslide, thus  
 480 | optimizing a selected objective function (OF). The model parameter set for which the  
 481 | OF assumes its best value is the optimization procedure output. The eight GOF  
 482 | indices presented in Table 1 were used in turn as OFs and, consequently, eight  
 483 | optimal parameters sets were provided as the calibration output (one for each  
 484 | optimised OF). This means that a GOF index selected in Table 1 becomes an OF  
 485 | when it is used as an objective function of the automatic calibration algorithm.  
 486 | In order to quantitatively analyze the model performances we implemented a three  
 487 | steps verification procedure (3SVP). Firstly, we evaluated the performances of each

Giuseppe Formetta 10/21/2016 3:57 PM  
 Deleted: t

Giuseppe Formetta 10/21/2016 3:57 PM  
 Deleted: in

Giuseppe Formetta 10/21/2016 3:57 PM  
 Deleted: ;

Giuseppe Formetta 10/21/2016 3:57 PM  
 Deleted: p

Giuseppe Formetta 10/21/2016 3:58 PM  
 Deleted: are

Giuseppe Formetta 10/21/2016 3:58 PM  
 Deleted: accurate

Giuseppe Formetta 10/21/2016 3:59 PM  
 Deleted: for

Giuseppe Formetta 10/21/2016 3:59 PM  
 Deleted: ing

Giuseppe Formetta 10/21/2016 3:59 PM  
 Deleted: of

Giuseppe Formetta 10/21/2016 4:00 PM  
 Deleted: optimal values.

Giuseppe Formetta 10/21/2016 4:01 PM  
 Deleted: t

Giuseppe Formetta 10/21/2016 4:01 PM  
 Deleted: To better clarify:

Giuseppe Formetta 10/21/2016 4:01 PM  
 Deleted: t

Giuseppe Formetta 10/21/2016 4:02 PM  
 Deleted: every

502 OF index for each model. We presented the results in the ROC plane in order to  
 503 assess what the OF index(es) was (where), whose optimization provided the best  
 504 model performances. Secondly, we verified wheatear each OF metric had its own  
 505 information content or wheatear it provided information analogous to other metrics  
 506 (and thus not essential).

507 Lastly, for each model, the sensitivity of each optimal parameter set was tested by  
 508 perturbing optimal parameters and by evaluating their effects on the GOF.

509

## 510 2.4 Site Description

511

512 The test site was located in Calabria, Italy, along the Salerno-Reggio Calabria  
 513 highway between Cosenza and Altilla municipalities, in the southern part of the Crati  
 514 basin (Figure 2). The mean annual precipitation is about 1200 mm, distributed  
 515 over approximately 100 rainy days, with a mean annual temperature of 16 °C.  
 516 Rainfall peaks occur from October to March, when mass wasting and severe water  
 517 erosion processes are triggered (Capparelli et al., 2012, Conforti et al., 2011, Iovine  
 518 et al., 2010).

519 In the study area the topographic elevation has an average value of around 450 m  
 520 a.s.l., with a maximum value of 730 m a.s.l. Slopes, computed from the 10 meters  
 521 resolution digital elevation model, range from 0° to 55°, while the average is about  
 522 26°.

523 The Crati Basin is a Pleistocene-Holocene extensional basin filled by clastic marine  
 524 and fluvial deposits (Vezzani, 1968; Colella et al., 1987; Fabbricatore et al., 2014).

525 The stratigraphic succession of the Crati Basin can be simply divided into two  
 526 sedimentary units as suggested by Lanzafame and Tortorici (1986). The first unit is a  
 527 Lower Pliocene succession of conglomerates and sandstones passing upward into a  
 528 silty clay (Lanzafame and Tortorici, 1986) second unit. This is a series of clayey  
 529 deposits grading upward into sandstones and conglomerates which refer to Emilian  
 530 and Sicilian, respectively (Lanzafame and Tortorici, 1986), as also suggested by  
 531 data provided by Young and Colella (1988).

532 In the study area the second unit outcrops. A topsoil of about 1.5 - 2.0 m lies on  
 533 sandy-gravelly and sandy deposits, which are generally well-stratified. Soils range  
 534 from Alfisols (i.e. highly mature soils) to Inceptisols and Entisols (i.e. poorly

Giuseppe Formetta 10/21/2016 4:02 PM  
 Deleted: single ...F index for each ... [18]

Giuseppe Formetta 10/21/2016 4:03 PM  
 Deleted: is ...as tested by perturb ... [19]

Giuseppe Formetta 10/2/2016 9:44 AM  
 Moved (insertion) [1]

Giuseppe Formetta 10/2/2016 9:44 AM  
 Deleted: 3.1

Giuseppe Formetta 10/2/2016 9:45 AM  
 Formatted: Font:Bold

Giuseppe Formetta 10/21/2016 4:03 PM  
 Deleted: portion...art of the Crati ... [20]

Giuseppe Formetta 10/21/2016 4:05 PM  
 Deleted: its

Giuseppe Formetta 10/3/2016 8:53 PM  
 Deleted: ...Colella et al., ... [21]

567 developed soils). Due to the combination of such climatic, geo-structural, and  
 568 geomorphological features the test site is one of the most landslide prone areas in  
 569 Calabria (Conforti et al., 2014; Carrara and Merenda, 1976; Iovine et al., 2006,).  
 570 Mass movements were analyzed from 2006 to 2013 by integrating aerial  
 571 photography interpretation acquired in 2006, 1:5000 scale topographic maps  
 572 analysis, and an extensive field survey.  
 573 All the data were digitized and stored in a GIS database (Conforti et al., 2014) and  
 574 the result was the map of occurred landslides, presented in Figure 2.D. Digital  
 575 elevation model, slope and total contributing area (TCA) maps are presented in  
 576 Figures 2, A, B, and C respectively. In order to perform model calibration and  
 577 verification, the dataset of occurred landslides was divided in two parts one used for  
 578 calibration (located at bottom of Figure 2.D) and one for validation (located in the  
 579 upper part of Figure 2.D). The landslide inventory map refers only to the initiation  
 580 area of the landslides. This leads to a fair comparison with the landslide models that  
 581 provide only the triggering point and does not include a runout model for landslides  
 582 propagation.

### 3 RESULTS AND DISCUSSION

586 The LSA presented in the paper was applied to the Salerno-Reggio Calabria  
 587 highway, between Cosenza and Altilia (southern Italy). Subsection 3.1 describes the  
 588 model parameters calibration and the model verification procedure; 3.2 presents the  
 589 model performance correlation assessment; 3.3 presents the robustness analysis of  
 590 the GOF indices used; and lastly, 3.4 presents the computation of the susceptibility  
 591 map.

#### 3.1 Model calibration and verification

Giuseppe Formetta 10/21/2016 4:08 PM  
 Deleted: f...i...ure 2,D. Digital ele... [22]  
 Giuseppe Formetta 10/2/2016 9:51 AM  
 Deleted: .  
 Giuseppe Formetta 10/2/2016 9:59 AM  
 Deleted: MODELING FRAMEWORK APPLICATION  
 Giuseppe Formetta 10/21/2016 4:10 PM  
 Deleted: is ...as applied for ...o th... [23]  
 Giuseppe Formetta 10/2/2016 9:44 AM  
**Moved up [1]: 3.1 Site Description**  
 The test site was located in Calabria, Italy, along the Salerno-Reggio Calabria highway between Cosenza and Altilia municipalities, in the southern portion of the Crati basin (Figure 2). The mean annual precipitation is about of 1200 mm, distributed on about 100 rainy days, and mean annual temperature of 16 °C. Rainfall peaks occur in the period October–March, during which mass wasting and severe water erosion processes are triggered (Capparelli et al., 2012, Conforti et al., 2011, Iovine et al., 2010).  
 In the study area the topographic elevation has an average value of around 450 m a.s.l., with a maximum value of 730 m a.s.l. Slope, computed from 10 meters resolution digital elevation model, range from 0° to 55°, while its average is about 26°.  
 The Crati Basin is a Pleistocene-Holocene extensional basin filled by clastic marine and fluvial deposits (Vezzani, 1968, Colella et al., 1987, Fabbriatore et al., 2014). The stratigraphic succession of the Crati Basin can be simply divided into two sedimentary units as suggested by Lanzafame and Tortorici, 1986. The first unit is a Lower Pliocene succession of conglomerates and sandstones passing upward into silty clays (Lanzafame and Tortorici, 1986) second unit. This is a succession of clayey deposits grading upward into sandstones and conglomerates referred to Emilian and Sicilian, respectively (Lanzafame and Tortorici, 1986), as also suggested by data provided by Young and Colella (1988). Mass movements were analyzed from 2006 to 2013 by integrating aerial photography interpretation acquired in 2006, 1:5000 scale topographic maps analysis, and extensive field survey.  
 All the data were digitized and stored in GIS database (Conforti et al., 2014) and the result was the map of occurred landslide presented in figure 2,D. Digital elevation model, slope and total contributing area (TCA) maps are [24]  
 Giuseppe Formetta 10/2/2016 9:44 AM  
 Deleted: 2...Models [25]

868

869 The three models presented in Section 2 were used to predict the landslide  
 870 susceptibility for the study area. Models parameters were optimized using each GOF  
 871 index presented in Table 1 in order to fit landslides of the calibration group. Table 2  
 872 presents the list of parameters that will be optimized, specifying their initial range of  
 873 variation, and the parameters kept constant during the simulation and their value.

Giuseppe Formetta 10/21/2016 4:13 PM  
 Deleted: s...ction 2 were applied ... [26]

874 The component PSO provides eight best parameter sets, one for each optimized  
 875 GOF indices. Values for each model (M1, M2 and M3) are presented in Table 3.  
 876 Optimal parameter sets differ slightly among the models and among the optimized  
 877 GOF indices for a given model. In addition a compensation effect between the  
 878 parameter values is evident. High values of friction angle are related to low cohesion  
 879 values; high values of critical rainfall are related to high values of soil resistance  
 880 parameters. For the model M1, the transmissivity value (74 m<sup>2</sup>/d) optimizing ACC is  
 881 much lower than the transmissivity values obtained by optimizing the other indices  
 882 (around 140 m<sup>2</sup>/d). Similar behavior was observed for the optimal rainfall value  
 883 which is 148 [mm/d] optimizing ACC, and around 70 [mm/d] optimizing the other  
 884 indices. For the model M2, the optimal transmissivity and rainfall values optimizing  
 885 CSI (10 [m<sup>2</sup>/d] and 95 [mm/d]), are much lower than the values obtained by  
 886 optimizing the other indices (around 50 [m<sup>2</sup>/d] and 250 [mm/d] in average). For the  
 887 model M3, on the other hand, optimal parameters present the same order of  
 888 magnitude for all the optimized indices. This suggests that the variability of the  
 889 optimal parameter values for models M1 and M2 could be due to compensate the  
 890 effects of important physical processes neglected by those models.

Giuseppe Formetta 10/21/2016 4:13 PM  
 Deleted: 8...best parameters...se ... [27]

891 Executing the models using the eight optimal parameters set, true positive rates and  
 892 false positive rates are computed by comparing the model output and actual  
 893 landslides for both the calibration and verification datasets. The results are  
 894 presented in Table 4, for all three models M1, M2 and M3. These points were  
 895 reported in the ROC plane to visualize the effects of the optimized objective function  
 896 on model performances in a unique graph. This procedure was repeated for the  
 897 three models. ROC planes, considering all the GOF indices and all three models, are  
 898 included in Appendix 2 both for the calibration and verification period. For models M2  
 899 and M3, it is clear that ACC, HSS, and CSI performed the worst. This is also true for

Giuseppe Formetta 10/21/2016 4:20 PM  
 Deleted: -...ositive -...ates and fa' ... [28]

940 | model M1, although, unlike M2 and M3, there is no clear separation between the  
 941 | performances provided by ACC, HSS, and CSI and the remaining indices.

Giuseppe Formetta 10/21/2016 4:23 PM  
 Deleted: even if...lthough, differer... [29]

942 | Among the results provided in Table 4, we focused on the GOF indices, whose  
 943 | optimization satisfies the condition:  $FPR < 0.4$  and  $TPR > 0.7$ . This choice was made in  
 944 | order to focus comments on the results exclusively for the GOF indices which  
 945 | provide acceptable model results and in order to heighten the readability of graphs.

Giuseppe Formetta 10/21/2016 4:24 PM  
 Deleted: our attention only ...n th... [30]

946 | Figure 3 presents three ROC planes, one for each model, with the optimized GOF  
 947 | indices that provide  $FPR < 0.4$  and  $TPR > 0.7$ . The results presented in Figure 3 and  
 948 | Table 4 show that: i) the optimization of AI, D2PC, SI and TSS achieves the best  
 949 | model performance in the ROC plane, which is verified for all three models; ii)  
 950 | performances increase as model complexity increases: moving from M1 to M3 points  
 951 | in the ROC plane approaches the perfect point ( $TPR=1$ ,  $FPR=0$ ); iii) by increasing  
 952 | the model complexity, good model results are achieved, not only in the calibration  
 953 | but also in the validation dataset. In fact, moving from M1 to M2 soil cohesion and  
 954 | soil properties were considered, and moving from M2 to M3 rainfall of a finite  
 955 | duration was used.

Giuseppe Formetta 10/21/2016 4:26 PM  
 Deleted: s...FPR<0.4 and TPR>0... [31]

956 | The first step of the 3SVP procedure highlights that the optimization of AI, D2PC, SI,  
 957 | and TSS provides the best performances irrespectively of the model used.

Giuseppe Formetta 10/21/2016 4:28 PM  
 Deleted: remarks ...hat the optimi... [32]

958 | Finally, it is important to consider the limitations of the models used for the current  
 959 | applications. Models M1 and M2 are not able to mimic the transient nature of  
 960 | precipitation and infiltration processes, and only M3 is able to account for the  
 961 | combined effect of storm duration and intensity in the triggering mechanism. In  
 962 | addition, in this study we neglected effects such as spatial rainfall variability, roads,  
 963 | and other engineering works.

### 965 | **3.2 Correlations assessment of the models performances**

Giuseppe Formetta 10/2/2016 9:52 AM  
 Deleted: 3...Correlations asses... [33]

967 | The second step in the procedure is to verify the information content of each  
 968 | optimized OF, checking whether it is the same as other metrics or it is particular  
 969 | feature of the optimized OF.

Giuseppe Formetta 10/3/2016 8:58 PM  
 Deleted: o...step of ...n the proce... [34]

970 | Executing a model using one of the eight parameters set (assuming, for example,  
 971 | the one obtained by optimizing CSI) enables all the remaining GOF indices to be  
 972 | computed, which we indicate as  $CSI_{CSI}$ ,  $ACC_{CSI}$ ,  $HSS_{CSI}$ ,  $TSS_{CSI}$ ,  $AI_{CSI}$ ,  $SI_{CSI}$ ,

Giuseppe Formetta 10/21/2016 4:30 PM  
 Deleted: let's assume...ssuming, (... [35]

1013 D2PC<sub>CSI</sub>, ES<sub>CSI</sub>, both for calibration and for verification dataset. Let us denote this  
 1014 vector with the name  $MP_{CSI}$ : the model performance ( $MP$ ) vector computed using the  
 1015 parameter set that optimizes CSI.  $MP_{CSI}$  has 16 elements, 8 for the calibration and 8  
 1016 for the validation dataset. Repeating the same procedure for all eight GOF indices it  
 1017 gives:  $MP_{ACC}$ ,  $MP_{ESI}$ ,  $MP_{SI}$ ,  $MP_{D2PC}$ ,  $MP_{TSS}$ ,  $MP_{AI}$ ,  $MP_{HS}$ . Figure 4 presents the  
 1018 correlation plots (Murdoch and Chow, 1996) between all  $MP$  vectors, for each model  
 1019 M1, M2 or M3. The matrix is symmetric with an ellipse at the intersection of row  $i$  and  
 1020 column  $j$ . The color is the absolute value of the correlation coefficient between the  
 1021  $MP_i$  and  $MP_j$  vectors. The eccentricity of the ellipse is scaled according to the  
 1022 correlation value: the more prominent it is, the less correlated are the vectors. If the  
 1023 ellipse leans towards the right, the correlation is positive, if it leans to the left, it is  
 1024 negative.

1025 All indices present a positive correlation with each other, irrespectively of the model  
 1026 used. In addition, strong correlations between the  $MP$  vectors of AI, D2PC, SI, and  
 1027 TSS are evident in Figure 4. This confirms that an optimization of AI, D2PC, SI, and  
 1028 TSS provides similar model performances, irrespectively of the model used. On the  
 1029 other hand, the remaining GOF indices give quite different information from the  
 1030 previous four indices, however their performance was worse in the first step of the  
 1031 analysis. Thus in the case study, using one of the four best GOFs is sufficient for the  
 1032 parameter estimation.

1033

### 1034 3.3 Models sensitivity assessment

1035

1036 In this step we focused on models M2 and M3 and performed a parameter sensitivity  
 1037 analysis. Let us consider model M2 and the optimal parameter set computed by  
 1038 optimizing the Critical Success Index (CSI). Also, considering the cohesion model  
 1039 parameter, the procedure evolves according to the following steps:

- 1040 • The starting parameter values are the optimal values derived from the
- 1041 optimization of the CSI index;
- 1042 • All the parameters except the analyzed parameter (cohesion) were kept
- 1043 constant and equal to the optimal parameter set;
- 1044 • 1000 random values of the analyzed parameter (cohesion) were selected
- 1045 from a uniform distribution with the lower and upper bound defined in Table 1.

Giuseppe Formetta 10/21/2016 4:31 PM

Deleted: Let's ...et us denote this ... [36]

Giuseppe Formetta 10/21/2016 4:34 PM

Deleted: among ...ith each other, ... [37]

Giuseppe Formetta 10/2/2016 9:52 AM

Deleted: 4

Giuseppe Formetta 10/21/2016 4:37 PM

Deleted: the ...odels M2 and M3 ... [38]

Giuseppe Formetta 10/21/2016 4:38 PM

Deleted: picked up

1080 With this procedure 1000 model parameter sets were defined and used to  
 1081 execute the model.

- 1082 • 1000 values of the selected GOF index (CSI), computed by comparing model  
 1083 outputs with the measured data, were used to compute a boxplot of the  
 1084 parameter C and optimized index CSI.

1085 The procedure was repeated for each parameter and for each optimized index.

1086 Results are presented in Figures 5 and 6 for models M2 and M3 respectively.

1087 Each column in the figures represents one optimized index and has a number of  
 1088 boxplots equal to the number of model parameters (5 for M2 and 6 for M3). Each  
 1089 boxplot represents the range of variation of the optimized index due to a particular  
 1090 change in the model parameters. The narrower the boxplot for a given optimized  
 1091 index, the less sensitive the model is to that parameter. For both M2 and M3, the  
 1092 parameter set obtained by optimizing AI and SI shows the least sensitive behavior  
 1093 for almost all the parameters. In this case a model parameter perturbation has little  
 1094 impact on the model's performances. However, the models with parameters  
 1095 obtained by optimizing ACC, TSS, and D2PC are the most sensitive to the  
 1096 parameter variations and this is reflected in much more evident changes in model  
 1097 performances. Finally, it is important to consider that the methodology used for  
 1098 evaluating the parameter sensitivity is based on changing the parameters one-at-  
 1099 time. Although this procedure facilitates an inter-comparison of the results (because  
 1100 the parameter sensitivity is computed with reference to the optimal parameter set), it  
 1101 is does not take into account simultaneous variations or interactions between  
 1102 parameters.

### 1104 3.4 Models selections and susceptibility maps

1106 The selection of the most appropriate model for computing landslide susceptibility  
 1107 maps is based on what we learn from the previous steps. In the first step we learn  
 1108 that i) the optimization of AI, D2PC, SI and TSS outperforms the remaining indices  
 1109 and ii) models M2 and M3 provide more accurate results than M1. The second step  
 1110 suggests that overall the model results obtained by optimizing AI, D2PC, SI and TSS  
 1111 are similar each other. Lastly, the third step shows that the model performance  
 1112 derived from the optimization of AI and SI is less sensitive to input variations than

- Giuseppe Formetta 10/21/2016 4:39 PM  
Deleted: were
- Giuseppe Formetta 10/21/2016 4:39 PM  
Deleted: of
- Giuseppe Formetta 10/21/2016 4:39 PM  
Deleted: 's
- Giuseppe Formetta 10/21/2016 4:40 PM  
Deleted: certain
- Giuseppe Formetta 10/21/2016 4:40 PM  
Deleted: change
- Giuseppe Formetta 10/21/2016 4:40 PM  
Deleted: is
- Giuseppe Formetta 10/21/2016 4:40 PM  
Deleted: less
- Giuseppe Formetta 10/21/2016 4:41 PM  
Deleted: does not influence much the model
- Giuseppe Formetta 10/21/2016 4:42 PM  
Deleted: On the contrary
- Giuseppe Formetta 10/21/2016 4:42 PM  
Deleted: h
- Giuseppe Formetta 10/21/2016 4:42 PM  
Deleted: re
- Giuseppe Formetta 10/21/2016 4:42 PM  
Deleted: s
- Giuseppe Formetta 10/21/2016 4:43 PM  
Deleted: ing
- Giuseppe Formetta 10/21/2016 4:43 PM  
Deleted: of
- Giuseppe Formetta 10/2/2016 9:52 AM  
Deleted: 5
- Giuseppe Formetta 10/21/2016 4:44 PM  
Deleted: more
- Giuseppe Formetta 10/21/2016 4:46 PM  
Deleted: s
- Giuseppe Formetta 10/21/2016 4:46 PM  
Deleted: compared
- Giuseppe Formetta 10/21/2016 4:46 PM  
Deleted: to
- Giuseppe Formetta 10/21/2016 4:46 PM  
Deleted: s
- Giuseppe Formetta 10/21/2016 4:47 PM  
Deleted: s
- Giuseppe Formetta 10/21/2016 4:47 PM  
Deleted: are
- Giuseppe Formetta 10/21/2016 4:47 PM  
Deleted: the
- Giuseppe Formetta 10/21/2016 4:47 PM  
Deleted: ble
- Giuseppe Formetta 10/21/2016 4:47 PM  
Deleted: compared to



1139 D2PC and TSS. This could be due to the formulation of AI and SI which gives much  
 1140 more weight to the true negative compared to D2PC and TSS.

1141 For our application, the model M3 with parameters obtained by optimizing D2PC was  
 1142 the most sensitive to the parameter variation avoiding an “insensitive” or flat  
 1143 response by changing the parameters values. A more sensitive couple model-  
 1144 optimal parameter set will in fact accommodate any parameters, input data, or  
 1145 measured data variations responding to these changes with a variation in model  
 1146 performance.

1147 We thus used the combination of model M3 with parameters obtained by optimizing  
 1148 D2PC in order to compute the final susceptibility maps in Figure 7. Categories of  
 1149 landslide susceptibility from classes 1 to 5 are assigned from low to high according  
 1150 to FS values (e.g. Huang et al., 2007): Class 1 ( $FS \leq 1.0$ ), Class 2 ( $1.0 < FS < 1.2$ ),  
 1151 Class 3 ( $1.2 < FS < 1.5$ ), Class 4 ( $1.5 < FS < 2.0$ ), Class 5 ( $FS \geq 2$ ).

#### 1153 4 Conclusions

1154  
 1155 We have presented a procedure to quantitatively calibrate, evaluate, and compare  
 1156 the performances of environmental models. The procedure was applied for the  
 1157 analysis of three landslides susceptibility models. It is made up of three steps: i)  
 1158 model parameters calibration, optimizing different GOF indices and models  
 1159 evaluation in the ROC plane; ii) computation of the degree of similarities between  
 1160 different model performances obtained by optimizing all the considered GOF indices;  
 1161 iii) evaluation of model sensitivity to parameter variations. The first step identifies the  
 1162 more appropriate OFs for the model parameter optimization. The second step  
 1163 verifies the information content of each optimized OF, checking whether it is  
 1164 analogous to other metrics or peculiar to the optimized OF. Finally the last step  
 1165 quantifies the relative influence of each model parameter on the model performance.

1166 The procedure was conceived as a model configuration of the hydrological system  
 1167 NewAge-JGrass; it integrates: i) three simplified physically based landslides  
 1168 susceptibility models; ii) a package for model evaluations based on pixel-by-pixel  
 1169 comparison of modeled and actual landslides maps; iii) models parameters  
 1170 calibration algorithms, and iv) the integration with the uDig open-source geographic  
 1171 information system for model input-output map management. The system is open-

- Giuseppe Formetta 10/21/2016 4:47 PM  
Deleted: behavior
- Giuseppe Formetta 10/21/2016 4:47 PM  
Deleted: that
- Giuseppe Formetta 10/21/2016 4:48 PM  
Deleted: In particular f
- Giuseppe Formetta 10/21/2016 4:48 PM  
Deleted: whit
- Giuseppe Formetta 10/21/2016 4:49 PM  
Deleted: eventual
- Giuseppe Formetta 10/21/2016 4:49 PM  
Deleted: of
- Giuseppe Formetta 10/21/2016 4:49 PM  
Deleted: For this reason w
- Giuseppe Formetta 10/21/2016 4:49 PM  
Deleted: the
- Giuseppe Formetta 10/21/2016 4:50 PM  
Deleted: for drawing
- Giuseppe Formetta 10/21/2016 4:50 PM  
Deleted: f
- Giuseppe Formetta 10/21/2016 4:50 PM  
Deleted: s
- Giuseppe Formetta 10/3/2016 9:07 PM  
Deleted: <
- Giuseppe Formetta 10/3/2016 9:07 PM  
Deleted: >
- Giuseppe Formetta 10/21/2016 4:50 PM  
Deleted: The paper presents
- Giuseppe Formetta 10/21/2016 4:51 PM  
Deleted: includes
- Giuseppe Formetta 10/21/2016 4:51 PM  
Deleted: 3
- Giuseppe Formetta 10/21/2016 4:51 PM  
Deleted: s
- Giuseppe Formetta 10/21/2016 4:52 PM  
Deleted: ex
- Giuseppe Formetta 10/21/2016 4:52 PM  
Deleted: s
- Giuseppe Formetta 10/21/2016 4:52 PM  
Deleted: s
- Giuseppe Formetta 10/3/2016 9:42 PM  
Deleted: .
- Giuseppe Formetta 10/21/2016 4:54 PM  
Deleted: has been
- Giuseppe Formetta 10/21/2016 4:54 PM  
Deleted: like
- Giuseppe Formetta 10/21/2016 4:54 PM  
Deleted: s
- Giuseppe Formetta 10/3/2016 9:32 PM  
Moved (insertion) [2]

1196 [source and available at \(https://github.com/formeppe\)](https://github.com/formeppe). It is integrated according to  
 1197 [the Object Modeling System standards which enables the user to easily integrate a](#)  
 1198 [generic landslide susceptibility model and use the complete framework presented in](#)  
 1199 [the paper, thus avoiding having to rewrite programming code.](#)

Giuseppe Formetta 10/21/2016 4:55 PM  
 Deleted: and this allows

1200 [The procedure was applied in a test case on the Salerno-Reggio Calabria highway](#)  
 1201 [and led to the following conclusions: 1\) the OFs AI, D2PC, SI, and TSS coupled with](#)  
 1202 [the models M2 and M3 provided the best performances among the eight metrics](#)  
 1203 [used in the calibration; 2\) the four selected OFs provided quite similar model](#)  
 1204 [performances in terms of MP vectors, i.e. one of them would be sufficient for the](#)  
 1205 [model application; 3\) M3 showed the best performance by optimizing the D2PC](#)  
 1206 [index. In fact M3 responded to parameter variations with changes in model](#)  
 1207 [performances.](#)

Giuseppe Formetta 10/21/2016 4:55 PM  
 Deleted: ing

Giuseppe Formetta 10/3/2016 9:32 PM  
 Deleted: The system will be helpful for decision makers that deal with risk management assessment and could be improved by adding new landslide susceptibility models or different types of model selection procedure.

Giuseppe Formetta 10/3/2016 9:33 PM  
 Deleted: This

Giuseppe Formetta 10/3/2016 9:36 PM  
 Deleted: was

1208 [In our application effective precipitation was calibrated because we were performing](#)  
 1209 [a landslide susceptibility analysis and it was useful for demonstrating the method.](#)  
 1210 [However, we are aware that for operational landslide early warning systems, rainfall](#)  
 1211 [constitutes a fundamental input of the predictive process. In addition, the analysis](#)  
 1212 [would profit from data on the rainfall that triggered the landslides, however such data](#)  
 1213 [are currently not available for the study area.](#)

Giuseppe Formetta 10/3/2016 10:14 PM  
 Deleted: the best model performances were provided by model M3 optimizing D2PC index.

Giuseppe Formetta 10/21/2016 4:57 PM  
 Deleted: the

Giuseppe Formetta 10/21/2016 4:57 PM  
 Deleted: we presented the

Giuseppe Formetta 10/21/2016 4:57 PM  
 Deleted: the

Giuseppe Formetta 10/21/2016 4:58 PM  
 Deleted: Moreover

1214 [We believe that our system would be useful for decision makers who deal with risk](#)  
 1215 [management assessments. It could be improved by adding new landslide](#)  
 1216 [susceptibility models or different types of model selection procedures.](#)

Giuseppe Formetta 10/21/2016 4:58 PM  
 Deleted: measured rainfall data that triggered the occurred landslides, but that such data are not available at the moment for the study area.

## 1218 ACKNOWLEDGMENTS

1219 [This research was funded by the PON Project No. 01\\_01503 "Integrated Systems for](#)  
 1220 [Hydrogeological Risk Monitoring, Early Warning and Mitigation Along the Main](#)  
 1221 [Lifelines", CUP B31H11000370005, within the framework of the National Operational](#)  
 1222 [Program for "Research and Competitiveness" 2007-2013. The authors would like to](#)  
 1223 [acknowledge the editor and the three reviewers \(Prof. M. Mergili and two unknown](#)  
 1224 [reviewers\) for providing insightful comments and improving the quality of the paper.](#)

Giuseppe Formetta 10/3/2016 9:32 PM  
 Moved up [2]: The system is open-source and available at (https://github.com/formeppe). It is integrated according the Object Modeling System standards and this allows the user to easily integrate a generic landslide susceptibility model and use the complete framework presented in the paper avoiding rewriting programming code. The system will be helpful for decision makers that deal with risk management assessment and could be improved by adding new landslide susceptibility models or different types of model selection procedure.

Giuseppe Formetta 10/21/2016 4:59 PM  
 Deleted: ACKNOWLEDGMENTS ... [39]

1225  
 1226  
 1227  
 1228

1267 **Acronyms table**

1268

3SVP	Three steps verification procedure
AI	Average Index
CSI	Critical success index
D2PC	Distance to perfect classification
ESI	Equitable success index
fn	False negative
fp	False positive
FPR	False positive rate
FS	Factor of safety
GIS	Geographic informatic system
GOF	Goodness of fit indices
HSS	Heidke skill score
LSA	Landslide susceptibility analysis
M1	Model for landslide susceptibility analysis proposed in Montgomery and Dietrich, 1994
M2	Model for landslide susceptibility analysis proposed in Park et al., 2013
M3	Model for landslide susceptibility analysis proposed in Rosso et al., 2006
MP	Model performances vector
OF	Objective function
OL	Observed landslide map
OMS	Object modeling system
PL	Predicted landslide map
PSO	Particle Swarm optimization
ROC	Receiver operating characteristic
SI	Success index
TCA	Total contributing area
tn	True negative
tp	True positive
TPR	True positive rate
TSS	True Skill Statistic

1269

1270

1271

1272

1273

1274

1275

1276

1277 **REFERENCES**

1278

- 1279 Abera W., A. Antonello, S. Franceschi, G. Formetta, R Rigon , "The uDig Spatial  
1280 Toolbox for hydro-geomorphic analysis" in GEOMORPHOLOGICAL  
1281 TECHNIQUES, v. 4, n. 1 (2014), p. 1-19. - URL:  
1282 [http://www.geomorphology.org.uk/sites/default/files/geom\\_tech\\_chapters/2.4.1\\_GI](http://www.geomorphology.org.uk/sites/default/files/geom_tech_chapters/2.4.1_GISToolbox.pdf)  
1283 [SToolbox.pdf](http://www.geomorphology.org.uk/sites/default/files/geom_tech_chapters/2.4.1_GISToolbox.pdf)
- 1284 Beguería, S. (2006). Validation and evaluation of predictive models in hazard  
1285 assessment and risk management. *Natural Hazards*, 37(3), 315-329.
- 1286 Bennett ND, Croke BF, Guariso G, Guillaume JH, Hamilton SH, Jakeman AJ,  
1287 Marsili-Libelli S, Newham LT, Norton JP, Perrin C, Pierce SA. Characterising  
1288 performance of environmental models. *Environmental Modelling & Software*. 2013  
1289 Feb 28;40:1-20.
- 1290 Borga, M., Dalla Fontana, G., & Cazorzi, F. (2002). Analysis of topographic and  
1291 climatic control on rainfall-triggered shallow landsliding using a quasi-dynamic  
1292 wetness index. *Journal of Hydrology*, 268(1), 56-71.
- 1293 Brabb, E.E., (1984). Innovative approaches to landslide hazard and risk mapping,  
1294 Proceedings of the 4th International Symposium on Landslides, 16–21 September,  
1295 Toronto, Ontario, Canada (Canadian Geotechnical Society, Toronto, Ontario,  
1296 Canada), 1:307–324
- 1297 Brenning, A. "Spatial prediction models for landslide hazards: review,  
1298 comparison and evaluation." *Natural Hazards and Earth System Science* 5,  
1299 no. 6 (2005): 853-862.
- 1300 Capparelli, G., & Versace, P. (2011). FLalR and SUSHI: two mathematical models  
1301 for early warning of landslides induced by rainfall. *Landslides*, 8(1), 67-79.
- 1302 Capparelli G, Iaquina P, Iovine GGR, Terranova OG, Versace P. Modelling the  
1303 rainfall-induced mobilization of a large slope movement in northern Calabria.  
1304 *Natural Hazards* 2012 ;61:247–256.
- 1305 [Carrara, A., Merenda, L., 1976. Landslide inventory in Northern Calabria, Southern](#)  
1306 [Italy. Geological Society of America Bulletin 87, 1153–1162](#)

- 1307 Casadei, M., Dietrich, W. E., & Miller, N. L. (2003). Testing a model for predicting the  
1308 timing and location of shallow landslide initiation in soil-mantled landscapes. *Earth*  
1309 *Surface Processes and Landforms*, 28(9), 925-950.
- 1310 Cascini, L., Bonnard, C., Corominas, J., Jibson, R., & Montero-Olarte, J. (2005).  
1311 Landslide hazard and risk zoning for urban planning and development. *Landslide*  
1312 *Risk Management*. Taylor and Francis, London, 199-235.
- 1313 Catani, F., Casagli, N., Ermini, L., Righini, G., & Menduni, G. (2005). Landslide  
1314 hazard and risk mapping at catchment scale in the Arno River basin. *Landslides*,  
1315 2(4), 329-342.
- 1316 Chung C-JF, Fabbri AG and van Westen CJ (1995) Multivariate regression analysis  
1317 for landslide hazard zonation. Carrara A and Guzzetti F (Eds.) Geographical  
1318 Information Systems in assessing natural hazards. Dordrecht, Kluwer Academic  
1319 Publishers. 5:107-34
- 1320 Colella A, De Boer PL, Nio SD. Sedimentology of a marine intermontane Pleistocene  
1321 Gilbert-type fan-delta complex in the Crati Basin, Calabria, southern Italy.  
1322 *Sedimentology* 1987;34:721–736.
- 1323 Conforti, M., Pascale, S., Robustelli, G., & Sdao, F. (2014). Evaluation of prediction  
1324 capability of the artificial neural networks for mapping landslide susceptibility in the  
1325 Turbolo River catchment (northern Calabria, Italy). *Catena*, 113, 236-250.
- 1326 Conforti M, Aucelli PPC, Robustelli G, Scarciglia F. Geomorphology and GIS  
1327 analysis for mapping gully erosion susceptibility in the Turbolo Stream catchment  
1328 (Northern Calabria, Italy). *Natural Hazards* 2011;56:881–898.
- 1329 Corominas J, Van Westen C, Frattini P, Cascini L, Malet JP, Fotopoulou S, Catani F,  
1330 Van Den Eeckhaut M, Mavrouli O, Agliardi F, Pitilakis K. Recommendations for the  
1331 quantitative analysis of landslide risk. *Bulletin of engineering geology and the*  
1332 *environment*. 2014 May 1;73(2):209-63.
- 1333 Dietrich, W. E., Bellugi, D. and Real De Asua, R. (2001) Validation of the Shallow  
1334 Landslide Model, SHALSTAB, for Forest Management, in *Land Use and*  
1335 *Watersheds: Human Influence on Hydrology and Geomorphology in Urban and*  
1336 *Forest Areas* (eds M. S. Wigmosta and S. J. Burges), American Geophysical  
1337 Union, Washington, D. C.. doi: 10.1029/WS002p0195
- 1338 David, O., Ascough II, J. C., Lloyd, W., Green, T. R., Rojas, K. W., Leavesley, G. H.,  
1339 & Ahuja, L. R. (2013). A software engineering perspective on environmental

- 1340 modeling framework design: The Object Modeling System. Environmental  
1341 Modelling & Software, 39, 201-213.
- 1342 Duan, Q., Sorooshian S., and Gupta V(1992): Effective and efficient global  
1343 optimization for conceptual rainfall-runoff models. Water Resources Research 28.4  
1344 (1992): 1015-1031.
- 1345 Duncan, J. M., and S. G. Wright (2005), Soil Strength and Slope Stability, 297 pp.,  
1346 New Jersey, John Wiley.
- 1347 Fabbriatore D, Robustelli G, Muto F. Facies analysis and depositional architecture  
1348 of shelf-type deltas in the Crati Basin (Calabrian Arc, south Italy). Boll. Soc. Geol.  
1349 It. 2014;133(1):131-148.
- 1350 Formetta, G., Mantilla, R., Franceschi, S., Antonello, A., & Rigon, R. (2011). The  
1351 JGrass-NewAge system for forecasting and managing the hydrological budgets at  
1352 the basin scale: models of flow generation and propagation/routing. Geoscientific  
1353 Model Development, 4(4), 943-955.
- 1354 Formetta, G., Antonello, A., Franceschi, S., David, O., & Rigon, R. (2014).  
1355 Hydrological modelling with components: A GIS-based open-source framework.  
1356 Environmental Modelling & Software, 55, 190-200.
- 1357 Formetta, G., Capparelli, G., Rigon, R., and Versace, P.: Physically based landslide  
1358 susceptibility models with different degree of complexity: calibration and  
1359 verification. International Environmental Modelling and Software Society (iEMSs).  
1360 7th Intl. Congress on Env. Modelling and Software, San Diego, CA, June 15-19,  
1361 USA, Daniel P. Ames, Nigel W.T. Quinn and Andrea E. Rizzoli (Eds.), 2014.  
1362 [http://www.iemss.org/sites/iemss2014/papers/iemss2014\\_submission\\_157.pdf](http://www.iemss.org/sites/iemss2014/papers/iemss2014_submission_157.pdf)
- 1363 [G. Formetta, G. Capparelli, and P. Versace , Modelling rainfall induced shallow](#)  
1364 [landslides in the Landslide Early Warning Integrated System project Slopes and](#)  
1365 [Geohazards. January 2015, 1747-1752. Available at:](#)  
1366 <http://www.icevirtuallibrary.com/doi/abs/10.1680/ecsmge.60678.vol4.260>
- 1367 [Formetta, G., Simoni, S., Godt, J. W., Lu, N., & Rigon, R. \(2016\). Geomorphological](#)  
1368 [control on variably saturated hillslope hydrology and slope instability. Water](#)  
1369 [Resources Research.](#)
- 1370 Frattini, P., Crosta, G., & Carrara, A. (2010). Techniques for evaluating the  
1371 performance of landslide susceptibility models. Engineering geology, 111(1), 62-  
1372 72.

- 1373 Guzzetti, Fausto, Alberto Carrara, Mauro Cardinali, and Paola Reichenbach.  
1374 "Landslide hazard evaluation: a review of current techniques and their  
1375 application in a multi-scale study, Central Italy." *Geomorphology* 31, no. 1  
1376 (1999): 181-216.
- 1377 Guzzetti, F., Reichenbach, P., Ardizzone, F., Cardinali, M., & Galli, M. (2006).  
1378 Estimating the quality of landslide susceptibility models. *Geomorphology*, 81(1),  
1379 166-184.
- 1380 Glade, T., & Crozier, M. J. (2005). A review of scale dependency in landslide hazard  
1381 and risk analysis. *Landslide hazard and risk*, Vol. 3, 75-138.
- 1382 Goodenough, D.J., Rossmann, K., Lusted, L.B., 1974. Radiographic applications of  
1383 receiver operating characteristic (ROC) analysis. *Radiology* 110, 89–95.
- 1384 Graham J (1984) Methods of slope stability analysis. In: Brunsdon D, Prior DB (eds)  
1385 Slope instability. Wiley, New York, pp 171–215
- 1386 Hay, L.E., G.H. Leavesley, M.P. Clark, S.L. Markstrom, R.J. Viger, and M. Umemoto  
1387 (2006). Step-Wise, Multiple-Objective Calibration of a Hydrologic Model for a  
1388 Snowmelt-Dominated Basin. *Journal of the American Water Resources*  
1389 *Association* 42:877-890, 2006
- 1390 Huang, J. C., Kao, S. J., Hsu, M. L., & Liu, Y. A. (2007). Influence of Specific  
1391 Contributing Area algorithms on slope failure prediction in landslide modeling.  
1392 *Natural Hazards and Earth System Science*, 7(6), 781-792.
- 1393 Lanzafame G, Tortorici L. La tettonica recente del Fiume Crati (Calabria). *Geografia*  
1394 *Fisica e Dinamica Quaternaria* 1984; 4:11-21.
- 1395 [Iovine, G., Petrucci, O., Rizzo, V., Tansi, C., 2006. The March 7th 2005 Cavallerizzo](#)  
1396 [\(Cerzeto\) landslide in Calabria—Southern Italy. Engineering geology for](#)  
1397 [tomorrow's cities—the 10th IAEG congress, Nottingham \(UK\), The Geological](#)  
1398 [Society of London, Paper number 785.](#)
- 1399 [Lee, S., Choi, J., & Min, K. \(2002\). Landslide susceptibility analysis and verification](#)  
1400 [using the Bayesian probability model. Environmental Geology, 43\(1-2\), 120-131.](#)
- 1401 Young J, Colella A. Calcareous nanofossils from the Crati Basin. In: Colella A.  
1402 (ed.), *Fan Deltas-Excursion Guidebook*. Università della Calabria, Cosenza, Italy.  
1403 79-96; 1988.

- 1404 Kennedy, J., and Eberhart R.(1995): Particle swarm optimization. Neural Networks,  
1405 1995. Proceedings., IEEE International Conference on. Vol. 4. Perth, WA. IEEE,  
1406 1995.
- 1407 Iovine GGR, Lollino P, Gariano SL, Terranova OG. Coupling limit equilibrium  
1408 analyses and real-time monitoring to refine a landslide surveillance system in  
1409 Calabria (southern Italy). Natural Hazards and Earth System Sciences 2010;  
1410 10:2341–2354.
- 1411 Iverson RM. 2000. Landslide triggering by rain infiltration. Water Resources  
1412 Research 36(7): 1897–1910
- 1413 Jolliffe, I. T., & Stephenson, D. B. (Eds.). (2012). Forecast verification: a  
1414 practitioner's guide in atmospheric science. University of Exeter, UK.  
1415 John Wiley & Sons.
- 1416 Lu, N., and J. Godt (2008), Infinite slope stability under steady unsaturated seepage  
1417 conditions, Water Resour. Res., 44, W11404, doi:10.1029/2008WR006976.
- 1418 Milledge, D. G., Bellugi, D., McKean, J. A., Densmore, A. L., & Dietrich, W. E.  
1419 (2014). A multidimensional stability model for predicting shallow landslide size and  
1420 shape across landscapes. *Journal of Geophysical Research: Earth Surface*,  
1421 119(11), 2481-2504.
- 1422 Montgomery, D. R., & Dietrich, W. E. (1994). A physically based model for the  
1423 topographic control on shallow landsliding. Water resources research, 30(4), 1153-  
1424 1171.
- 1425 Murdoch, D. J., & Chow, E. D. (1996). A graphical display of large correlation  
1426 matrices. *The American Statistician*, 50(2), 178-180.
- 1427 Naranjo, J.L., van Westen, C.J. and Soeters, R. (1994) Evaluating the use of training  
1428 areas in bivariate statistical landslide hazard analysis: a case study in Colombia.  
1429 ITC Journal, 3:292-300.
- 1430 Pepe, M.S., 2003. The Statistical Evaluation of Medical Tests for Classification and  
1431 Prediction. Oxford University Press, New York.
- 1432 Park, N. W. (2011). Application of Dempster-Shafer theory of evidence to GIS-  
1433 based landslide susceptibility analysis. *Environmental Earth Sciences*,  
1434 62(2), 367-376.



- 1435 Park, H. J., Lee, J. H., & Woo, I. (2013). Assessment of rainfall-induced shallow  
1436 landslide susceptibility using a GIS-based probabilistic approach. *Engineering*  
1437 *Geology*, 161, 1-15.
- 1438 [Pradhan, B. \(2011\). An assessment of the use of an advanced neural network model](#)  
1439 [with five different training strategies for the preparation of landslide susceptibility](#)  
1440 [maps. \*Journal of Data Science\*, 9\(1\), 65-81.](#)
- 1441 [Pradhan, B. \(2013\). A comparative study on the predictive ability of the decision tree,](#)  
1442 [support vector machine and neuro-fuzzy models in landslide susceptibility](#)  
1443 [mapping using GIS. \*Computers & Geosciences\*, 51, 350-365.](#)
- 1444 Provost, F., Fawcett, T., 2001. Robust classification for imprecise environments.  
1445 *Machine Learning* 42 (3), 203–231.
- 1446 Rosso, R., M. C. Rulli, and G. Vannucchi (2006), A physically based model for the  
1447 hydrologic control on shallow landsliding, *Water Resour. Res.*, 42, W06410,  
1448 doi:10.1029/2005WR004369.
- 1449 Sidle, R. C., & Ochiai, H. (2006). *Landslides: processes, prediction, and land*  
1450 *use* (Vol. 18). Washington, DC 20009, USA. American Geophysical Union.
- 1451 Simoni, S., Zanotti, F., Bertoldi, G., and Rigon, R. (2008): Modeling the probability of  
1452 occurrence of shallow landslides and channelized debris flows using GEOtop-FS,  
1453 *Hydrol. Process.*, 22, 532{545,
- 1454 Vezzani L. I terreni plio-pleistocenici del basso Crati (Cosenza). *Atti dell'Accademia*  
1455 *Gioenia di Scienze Naturali di Catania* 6:28–84; 1968.
- 1456 Vrugt, J. A., C. J. F. ter Braak, M. P. Clark, J. M. Hyman, and B. A. Robinson (2008),  
1457 Treatment of input uncertainty in hydrologic modeling: Doing hydrology backward  
1458 with Markov chain Monte Carlo simulation, *Water Resour. Res.*, 44, W00B09,  
1459 doi:10.1029/2007WR006720.
- 1460  
1461  
1462  
1463  
1464  
1465  
1466  
1467

1468 **Table 1:** Indices of goodness of fit for comparison between actual and predicted  
 1469 landslide.  
 1470

Giuseppe Formetta 10/5/2016 1:41 PM

Deleted: .

... [40]

Name	Definition	Range	Optimal value
Critical success index (CSI)	$CSI = \frac{tp}{tp+fp+fn}$	[0, 1]	1.0
Equitable success index (ESI)	$ESI = \frac{tp-R}{tp+fp+fn-R}$ $R = \frac{(tp+fn) \cdot (tp+fp)}{tp+fn+fp+tn}$	[-1/3, 1]	1.0
Success Index (SI)	$SI = \frac{1}{2} \cdot \left( \frac{tp}{tp+fn} + \frac{tn}{fp+tn} \right)$	[0, 1]	1.0
Distance to perfect classification (D2PC)	$D2PC = \sqrt{(1-TPR)^2 + FPR^2}$ $TPR = \frac{tp}{tp+fn}$ $FPR = \frac{fp}{fp+tn}$	[0, 1]	0.0
Average Index (AI)	$AI = \frac{1}{4} \left( \frac{tp}{tp+fn} + \frac{tp}{tp+fp} + \frac{tn}{fp+tn} + \frac{tn}{fn+tn} \right)$	[0, 1]	1.0
True skill statistic (TSS)	$TSS = \frac{(tp \cdot tn) - (fp \cdot fn)}{(tp+fn) \cdot (fp+tn)}$	[-1, 1]	1.0
Heidke skill score (HSS)	$HSS = \frac{2 \cdot (tp \cdot tn) - (fp \cdot fn)}{(tp+fn) \cdot (fn+tn) + (tp+fp) \cdot (fp+tn)}$	[-∞, 1]	1.0
Accuracy (ACC)	$ACC = \frac{(tp+tn)}{(tp+fn+fp+tn)}$	[0, 1]	1.0

1471

1472

1473

1474

1475

1476

1477

1478

1479

1480

1481

1482

1485 **Table 2:** Optimised models' parameters values

1486

Model Parameters	Constant Value	Range value
Soil Depth [m]	-	[0.8; 5.0]
Transmissivity [m <sup>2</sup> /d]	-	[10; 150]
Soil/water density ratio	-	[1.8; 2.8]
Friction Angle [°]	-	[11; 40]
Rainfall [mm/d]	-	[50; 300]
Soil Cohesion [kPa]	-	[0; 50]
Degree Of Saturation [-]	0.5	-
Soil Porosity [-]	0.5	-
Rainfall Duration [d]	-	[0.1; 3.0]

1487

1488

1489

1490

1491

1492

1493

1494

1495

1496

1497

1498

1499

1500

1501

1502

1503

1504

1505

1506

1507

1508

1509 **Table 3:** Optimal parameter sets output of the optimization procedure of each GOF  
 1510 indices in turn. Results are presented for each model (M1, M2 and M3).

1511  
 1512  
 1513

Model: M1								
Optimised Index	AI	HSS	TSS	D2PC	SI	ESI	CSI	ACC
Soil Depth [m]	1.32	1.85	1.44	2.80	1.36	2.62	2.42	2.01
Transmissivity [m <sup>2</sup> /d]	140.24	146.31	142.68	137.10	147.69	144.66	136.73	74.74
Soil/water density ratio [-]	2.61	2.56	2.77	2.71	2.78	2.79	2.63	2.72
Friction Angle [°]	24.20	32.40	22.50	23.10	22.40	29.50	29.50	38.30
Rainfall [mm/d]	85.38	53.30	71.36	50.00	52.69	69.19	61.35	141.80

1514

Model: M2								
Optimised Index	AI	HSS	TSS	D2PC	SI	ESI	CSI	ACC
Transmissivity [m <sup>2</sup> /d]	65.43	33.22	80.45	38.22	84.54	33.24	10.70	55.76
Cohesion [kPa]	25.17	49.63	49.42	16.94	30.01	41.24	44.58	46.85
Friction Angle [°]	29.51	38.38	20.01	32.30	24.57	33.78	35.68	34.96
Rainfall [mm/d]	236.14	293.44	270.42	153.61	294.70	298.44	95.35	299.01
Soil/water density ratio [-]	2.11	2.40	2.06	2.44	2.77	2.17	2.55	2.19
Soil Depth [m]	2.35	1.68	2.38	2.44	2.74	1.12	1.37	1.12

1515

Model: M3								
Optimised Index	AI	HSS	TSS	D2PC	SI	ESI	CSI	ACC
Transmissivity [m <sup>2</sup> /d]	30.95	26.55	47.03	36.31	57.28	25.84	31.60	48.71
Cohesion [kPa]	36.88	44.33	28.51	31.60	45.46	41.80	32.05	37.09
Friction Angle [°]	19.55	36.44	27.80	29.70	21.46	33.27	36.47	38.50
Rainfall [mm/d]	248.77	230.08	258.82	201.71	299.90	291.32	273.03	193.02
Soil/water density ratio [-]	2.40	2.57	2.08	2.80	2.65	2.63	2.61	2.44
Soil Depth [m]	1.84	1.42	2.23	2.92	2.85	1.17	1.13	1.15
Rainfall Duration [d]	0.12	1.78	1.24	1.96	1.24	0.39	1.30	1.98

1516

1517

1518

1519

1520

1521 **Table 4:** Results in term of true-positive rate (TPR) and false-positive rate (FPR), for  
 1522 each model (M1, M2 and M3), for each optimised GOF index and for both calibration  
 1523 (CAL) and verification (VAL) dataset. In bold are shown the rows for which the  
 1524 condition  $FPR < 0.4$  and  $TPR > 0.7$  is verified.

1525

Period	Optim. Index	MODEL: M1		MODEL: M2		MODEL: M3	
		FPR	TPR	FPR	TPR	FPR	TPR
CAL	ACC	0.04	0.12	0.03	0.12	0.03	0.13
<b>CAL</b>	<b>AI</b>	<b>0.29</b>	<b>0.70</b>	<b>0.35</b>	<b>0.79</b>	<b>0.38</b>	<b>0.82</b>
CAL	CSI	0.17	0.48	0.10	0.36	0.09	0.32
<b>CAL</b>	<b>D2PC</b>	<b>0.32</b>	<b>0.72</b>	<b>0.32</b>	<b>0.76</b>	<b>0.32</b>	<b>0.75</b>
CAL	ESI	0.17	0.48	0.43	0.82	0.09	0.36
CAL	HSS	0.12	0.35	0.09	0.35	0.09	0.35
<b>CAL</b>	<b>SI</b>	<b>0.34</b>	<b>0.74</b>	<b>0.39</b>	<b>0.85</b>	<b>0.39</b>	<b>0.86</b>
<b>CAL</b>	<b>TSS</b>	<b>0.34</b>	<b>0.73</b>	<b>0.39</b>	<b>0.83</b>	<b>0.37</b>	<b>0.82</b>
VAL	ACC	0.05	0.12	0.03	0.12	0.03	0.10
VAL	AI	0.26	0.56	0.31	0.69	<b>0.34</b>	<b>0.72</b>
VAL	CSI	0.17	0.39	0.09	0.31	0.08	0.29
VAL	D2PC	0.29	0.59	0.28	0.67	0.28	0.66
VAL	ESI	0.17	0.39	0.41	0.76	0.09	0.30
VAL	HSS	0.12	0.30	0.09	0.30	0.09	0.30
VAL	SI	0.30	0.61	<b>0.37</b>	<b>0.75</b>	<b>0.39</b>	<b>0.76</b>
VAL	TSS	0.30	0.62	<b>0.35</b>	<b>0.74</b>	<b>0.34</b>	<b>0.71</b>

1526

1527

1528

1529

1530

1531

1532

1533

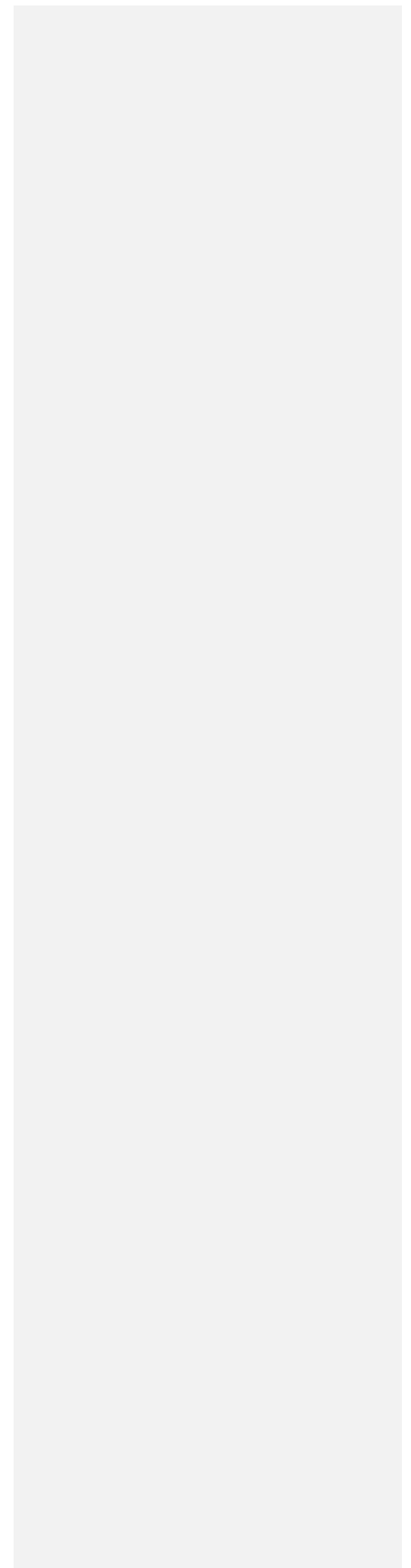
1534

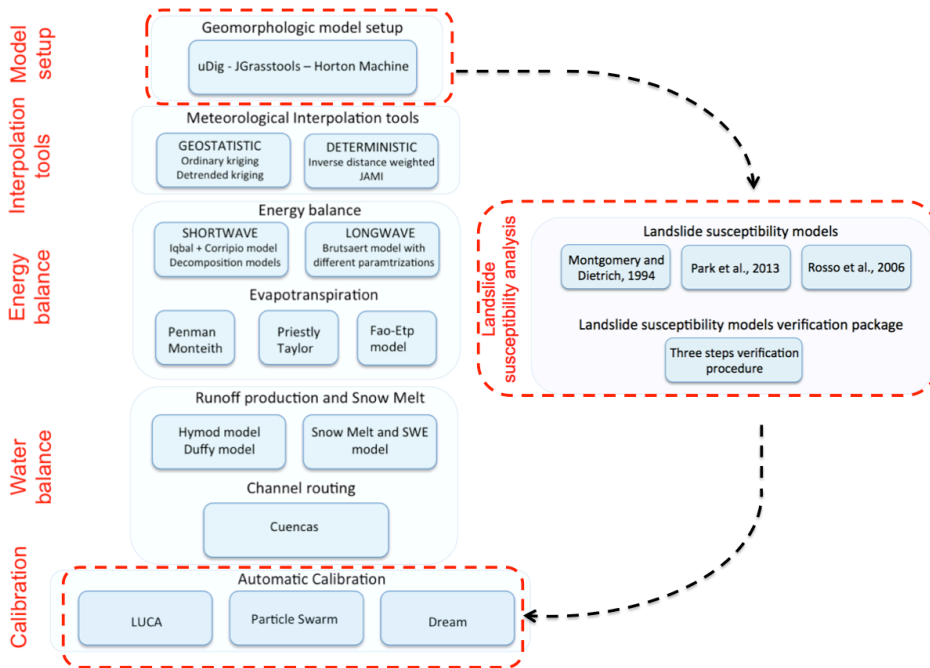
1535

1536

1537

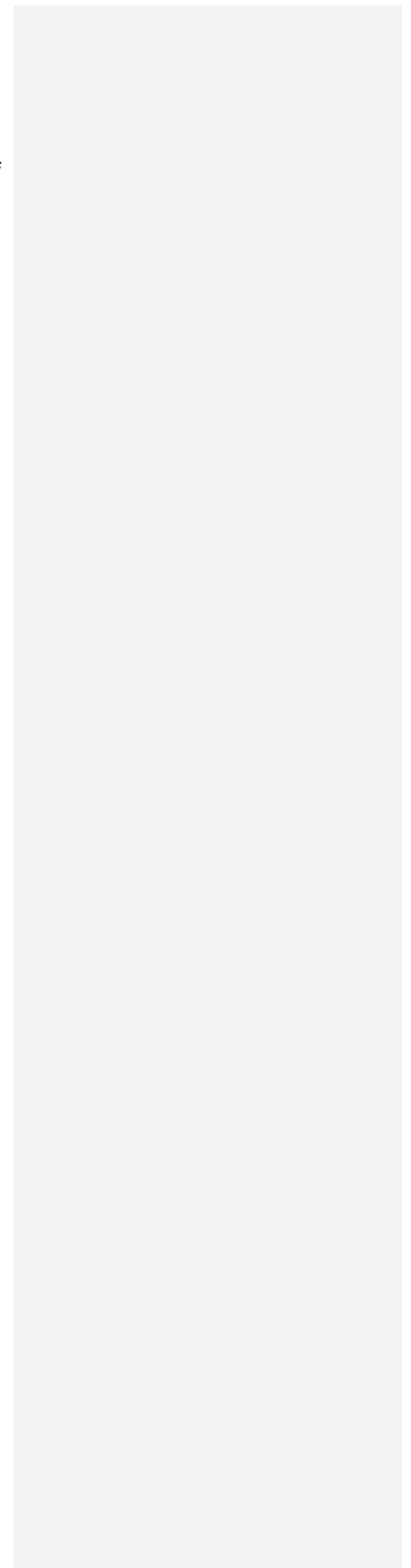
1538 **Figure 1:** Integration of the Landslide susceptibility analysis system in  
1539 NweAge-JGrass hydrological model.





1540  
 1541  
 1542  
 1543  
 1544  
 1545  
 1546  
 1547  
 1548  
 1549  
 1550  
 1551  
 1552  
 1553  
 1554  
 1555

1556 **Figure 2:** Test site. A) Digital elevation model (DEM) [m], B) slope [-] expressed as  
1557 tangent of the angle, C) total contributing area (TCA) expressed as number of  
1558 draining cells and D) Map of actual landslides.





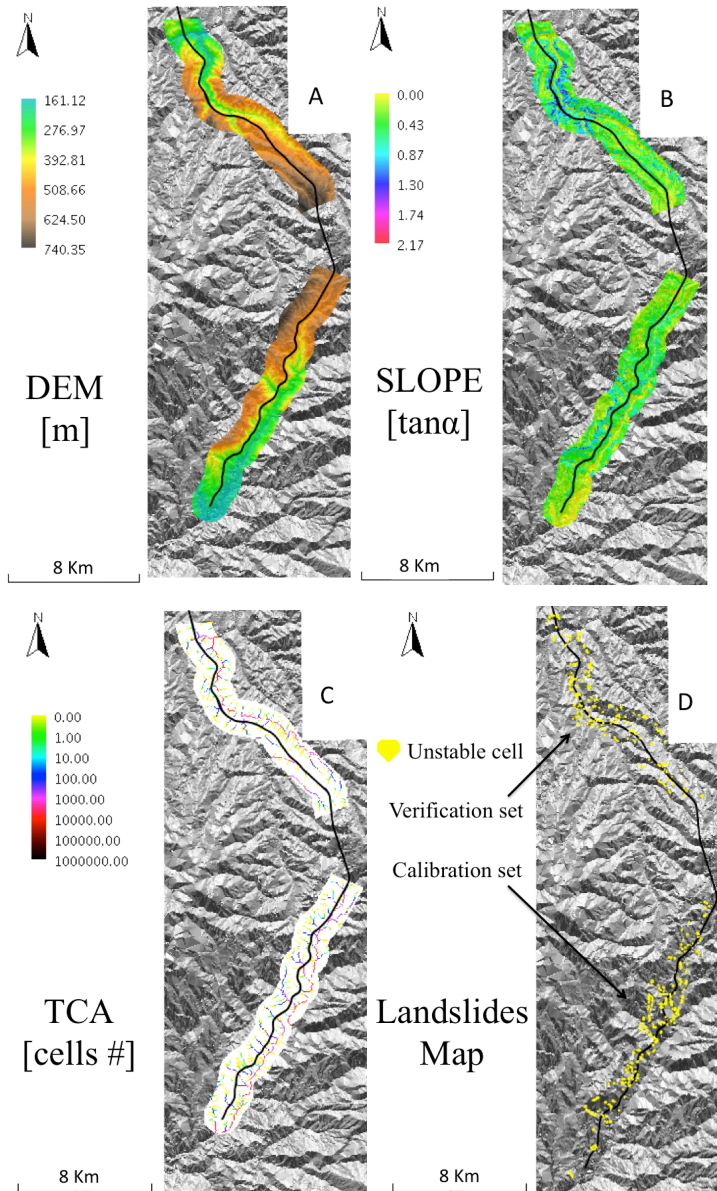


**Figure 3:** Models' performances results in the ROC plane for M1, M2 and M3. Only GOF indices whose optimization provides  $FPR < 0.4$  and  $TPR > 0.7$  were reported.

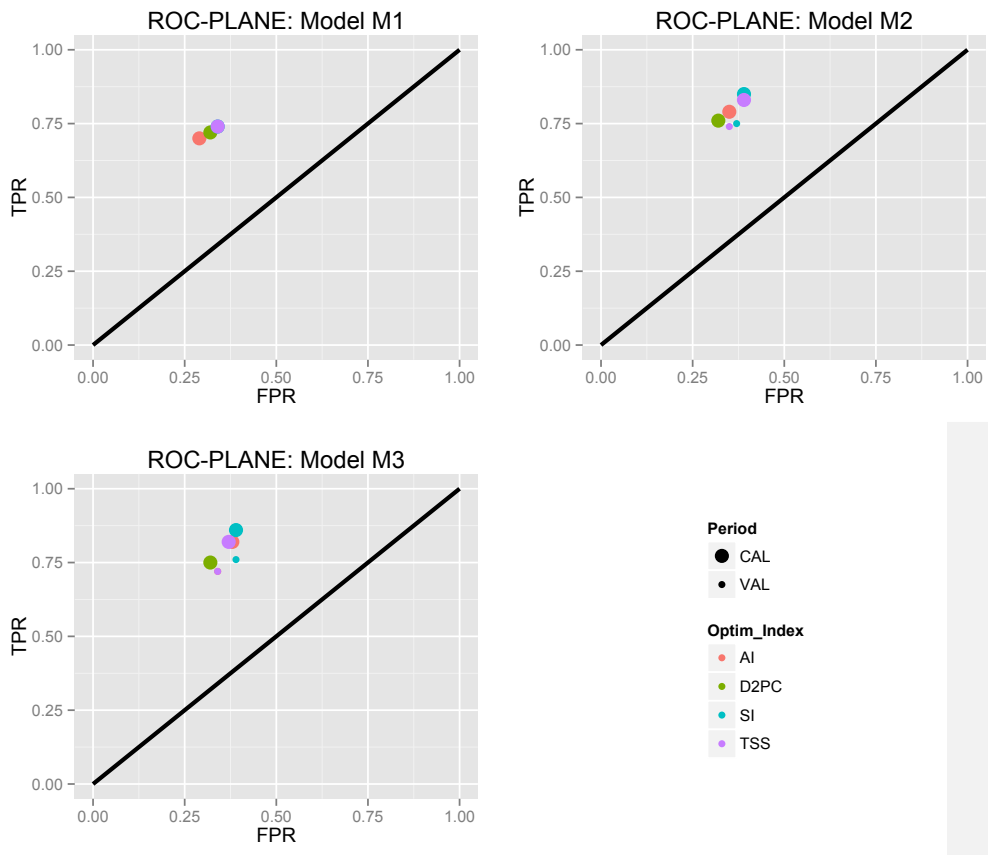


**Figure 4:** Correlation plot between models' performance (MP) vector computed by optimizing all GOF indices in turn. Results are reported for each model: M1, M2 and M3.

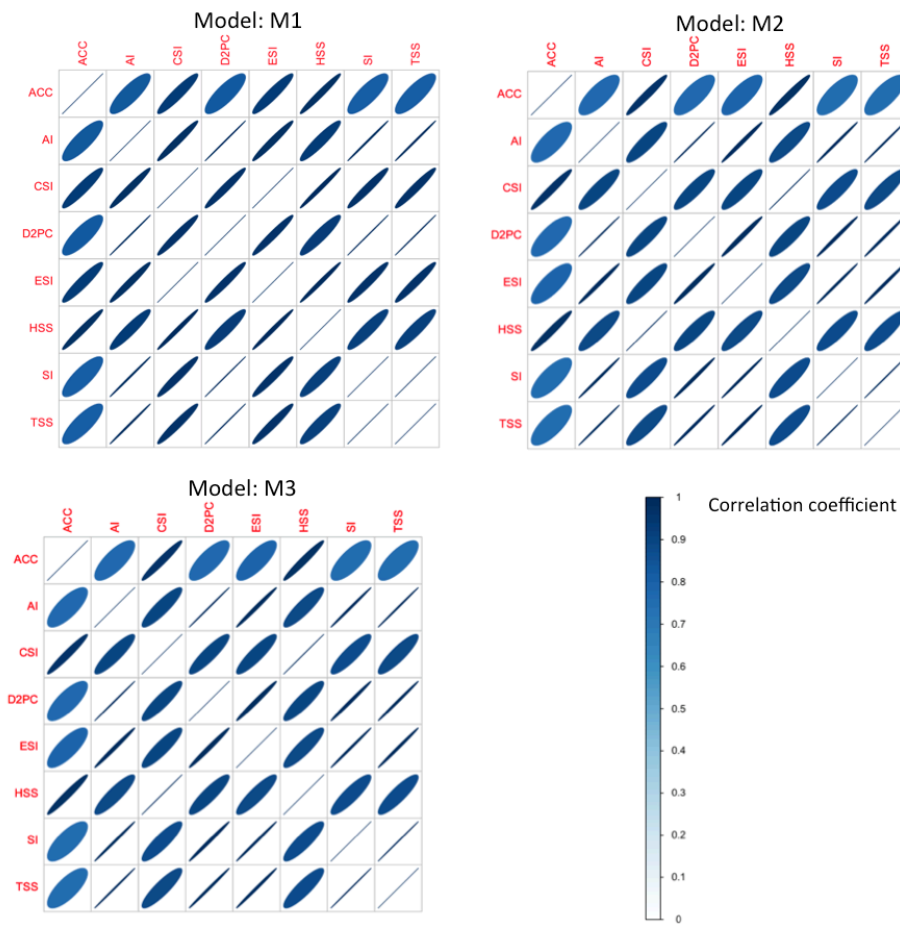


Figure 5: Model M2 parameters sensitivity analysis.

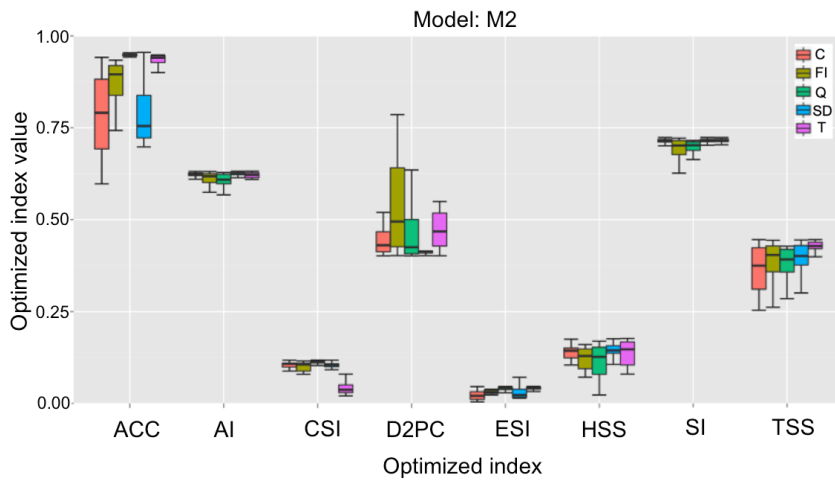
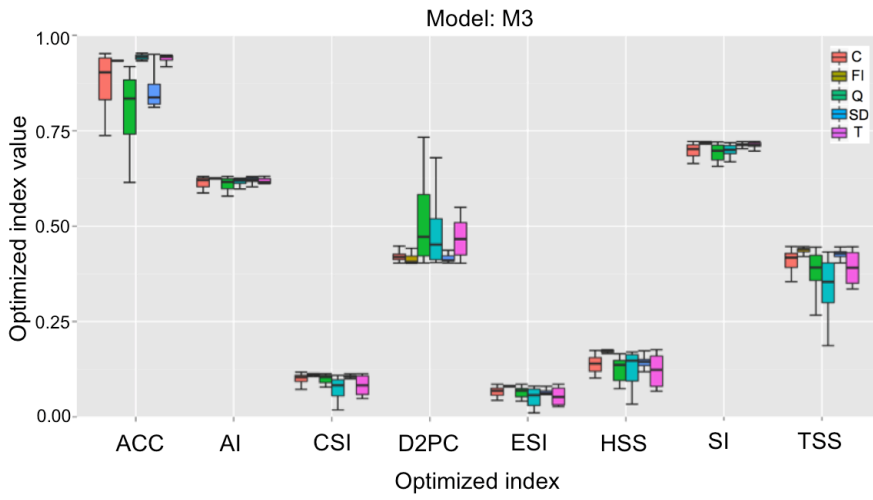
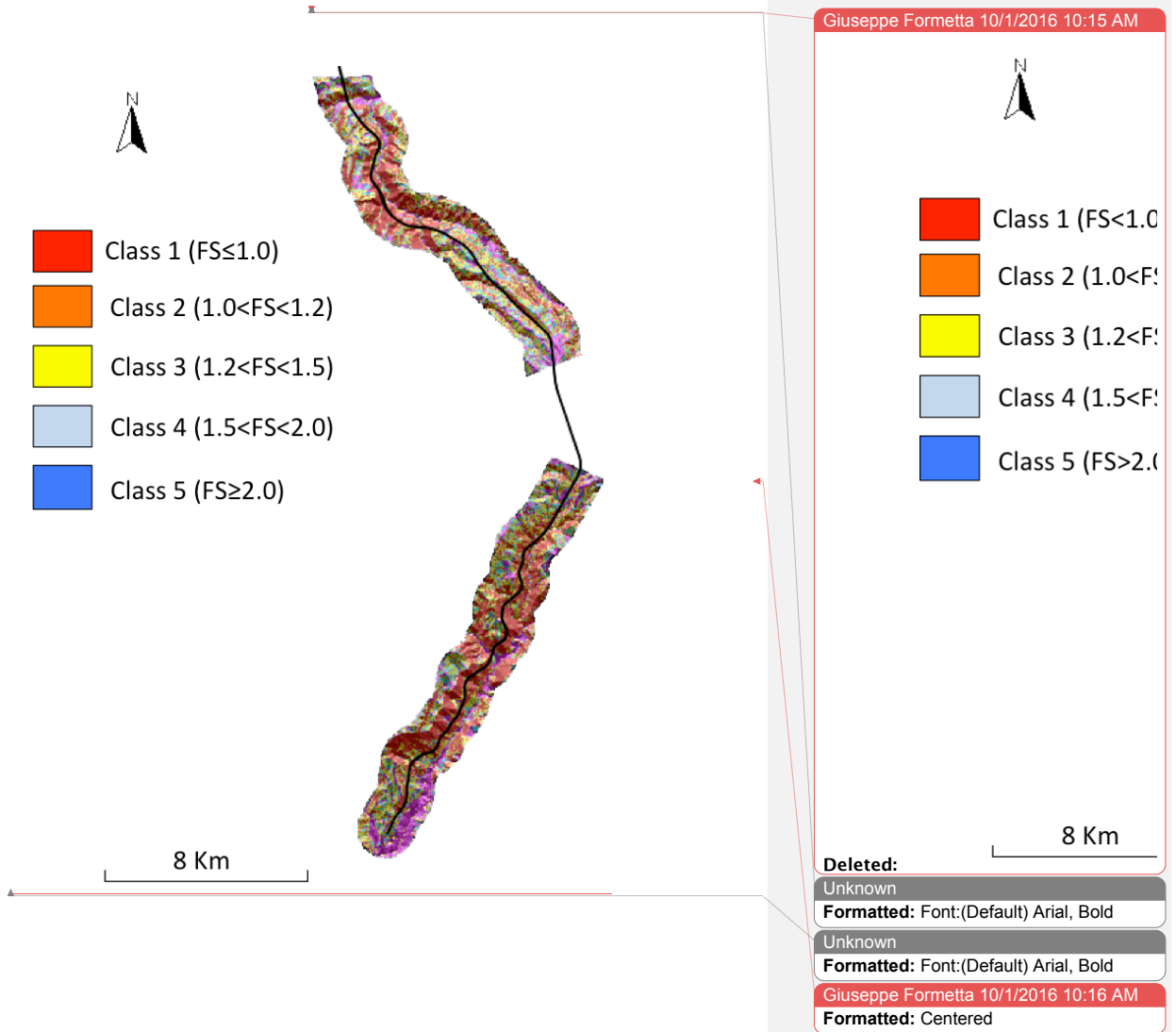


Figure 6: Model M3 parameters sensitivity analysis.



**Figure 7:** Landslide susceptibility maps using model M3 and parameter set obtained by optimising D2PC.



## Appendix 1

### 1.2 Critical success index (CSI)

CSI, eq. (2), is the number of correct detected landslide pixels (tp), divided by the sum of tp, fn and fp. CSI is also named threat score. It range between 0 and 1 and its best value is 1. It penalizes both fn and fp.

$$CSI = \frac{tp}{tp+fp+fn} \quad (2)$$

### 1.3 Equitable success index (ESI)

ESI, eq. (3), contrarily to CSI, is able to take into account the true positives associated with random chance (R). ESI ranges between -1/3 and 1. Value 1 indicates perfect score.

$$ESI = \frac{tp-R}{tp+fp+fn-R} \quad (3)$$

$$R = \frac{(tp+fn) \cdot (tp+fp)}{tp+fn+fp+tn} \quad (4)$$

### 1.4 Success index (SI)

SI, eq.(5), equally weight True positive rate (eq. 6) and specificity defined as 1 minus false positive rate (FPR), eq. (7). SI varies between 0 and 1 and its best value is 1. SI is also named modified success rate.

$$SI = \frac{1}{2} \cdot \left( \frac{tp}{tp + fn} + \frac{tn}{fp + tn} \right) = \frac{1}{2} \cdot (TPR + \text{specificity}) \quad (5)$$

$$TPR = \frac{tp}{tp + fn} \quad (6)$$

$$FPR = \frac{fp}{fp + tn} \quad (7)$$

### 1.5 Distance to perfect classification (D2PC)

D2PC is defined in eq. (8). It measures the distance, in the plane FPR-TPR between an ideal perfect point of coordinates (0,1) and the point of the tested model (FPR,TPR). D2PC ranges in 0-1 and its best value are 0.

$$D2PC = \sqrt{(1 - TPR)^2 + FPR^2} \quad (8)$$

### 1.6 Average Index (AI)

AI, eq. (9), is the average value between four different indices: i) TPR, ii) Precision, iii) the ratio between successfully predicted stable pixels (tn) and the total number of actual stable pixels (fp+tn) and iv) the ratio between successfully predicted stable pixels (tn) and the number of simulated stable cells (fn+tn).

$$AI = \frac{1}{4} \left( \frac{tp}{tp + fn} + \frac{tp}{tp + fp} + \frac{tn}{fp + tn} + \frac{tn}{fn + tn} \right) \quad (9)$$

### 1.7 Heidke skill score (HSS)



The fundamental idea of a generic skill score measure is to quantify the model performance respect to set of control or reference model. Fixed a measure of model accuracy  $M_a$ , the skill score formulation is expressed in eq. (10):

$$SS = \frac{M_a - M_c}{M_{opt} - M_c} \quad (10)$$

where  $M_c$  is the control or reference model accuracy and  $M_{opt}$  is the perfect model accuracy.

SS assumes positive and negative value, if the tested model is perfect  $M_a = M_{opt}$  and  $SS=1$ , if the tested model is equal to the control model than  $M_a = M_c$  and  $SS=0$ .

The marginal probability of a predicted unstable pixel is  $(tp+fp)/n$  where  $n$  is the total number of pixels  $n=tp+fn+fp+tn$ . The marginal probability of a landslided unstable pixel is  $(tp+fn)/n$ .

The probability of a correct yes forecast by chance is:  $P1 = (tp+fp) (tp+fn)/n^2$ . The probability of a correct no forecast by chance is:  $P2 = (tn+fp) (tn+fn)/n^2$ .

In the HSS, eq. (11), the control model is a model that forecast by chance:  $M_c = P1 + P2$ , the measure of accuracy is the Accuracy (ACC) defined in eq. (12), and the  $M_{opt}=1$ .

$$HSS = \frac{2 \cdot (tp \cdot tn) - (fp \cdot fn)}{(tp + fn) \cdot (fn + tn) + (tp + fp) \cdot (fp + tn)} \quad (11)$$

$$ACC = \frac{tp + tn}{tp + fn + fp + tn} \quad (12)$$

The range of the HSS is  $-\infty$  to 1. Negative values indicate that the model provides no better results of a random model, 0 means no model skill, and a perfect model obtains a HSS of 1. HSS is also named as Cohen's kappa.

### 1.8 True Skill Statistic (TSS)

TSS, eq. (13), is the difference between the hit rate and the false alarm rate. It is also named Hanssen & Kuipper's Skill Score and Pierce's Skill Score. It ranges between -1 and 1 and its best value is 1. TSS equal -1 indicates that the model provides no better results of a random model. A TSS equal 0 indicates an indiscriminate model.

TSS measures the ability of the model to distinguish between landslided and non-landslided pixels. If the number of  $t_n$  is large the false alarm value is relatively overwhelmed. If  $t_n$  is large, as happens in landslides maps, FPR tends to zero and TSS tends to TPR. A problem of TSS is that it treats the hit rate and the false alarm rate equally, irrespective of their likely differing consequences.

$$TSS = \frac{(tp \cdot tn) - (fp \cdot fn)}{(tp + fn) \cdot (fp + tn)} = TPR - FPR \quad (13)$$

TSS is similar to Heidke, except the constraint on the reference forecasts is that they are constrained to be unbiased.

## Appendix 2

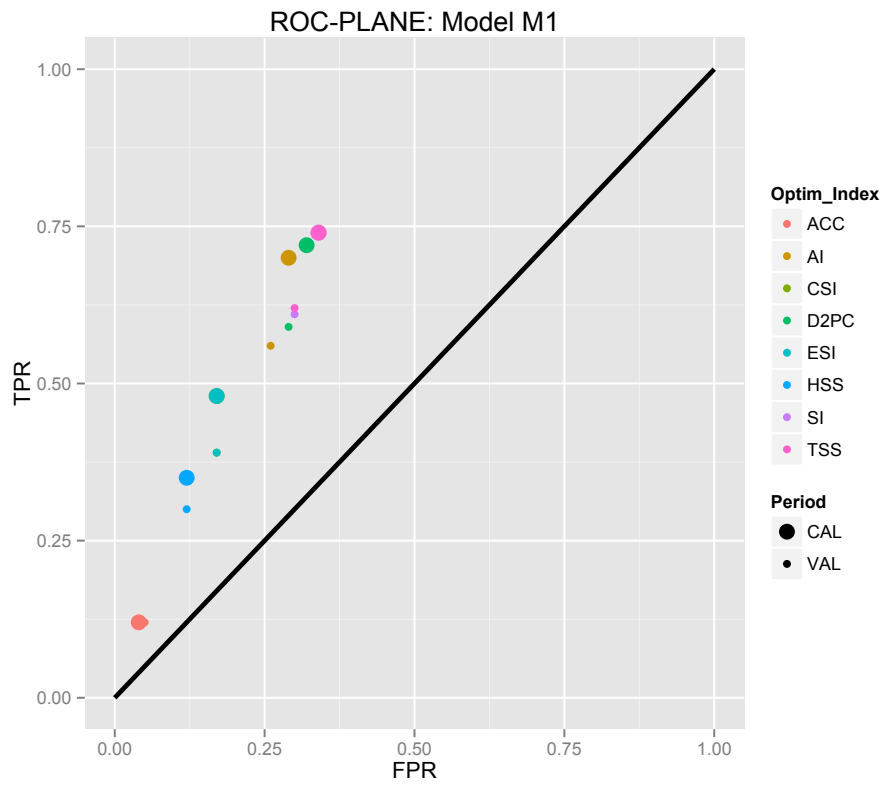


Figure A2-1: Models' performances results in the ROC plane for M1.

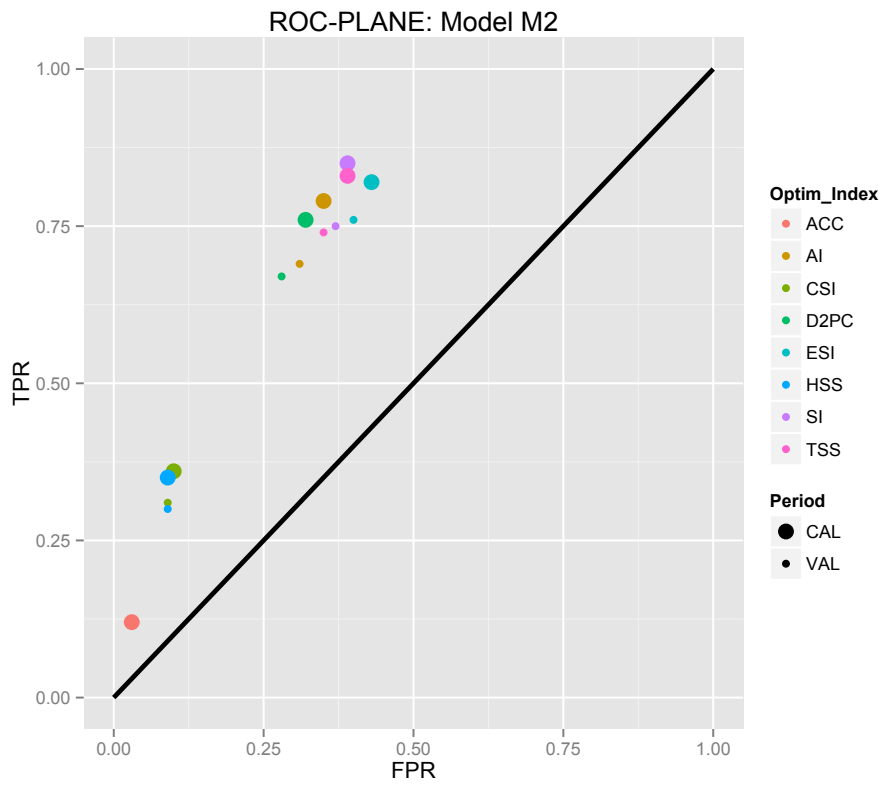


Figure A2-2: Models' performances results in the ROC plane for M2.

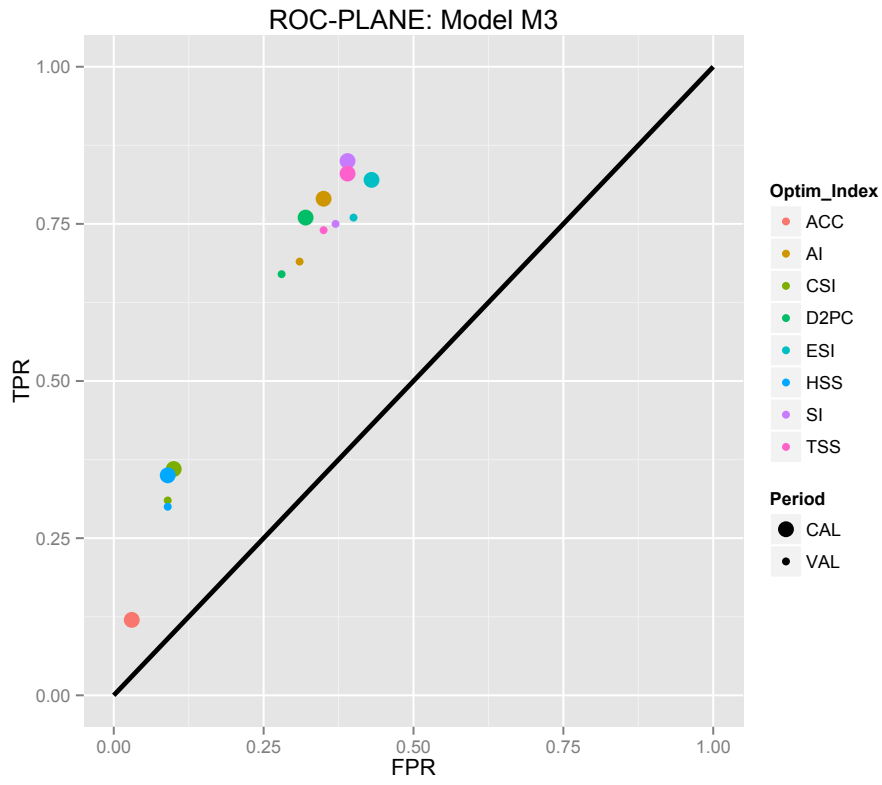


Figure A2-3: Models' performances results in the ROC plane for M3.

